2013-07-15

Model-Following Control for a Helicopter with Suspended Load in Low Velocity Forward Flight

Serpas Siguenza, Jose

THE UNIVERSITY OF CALGARY

Model-Following Control for a Helicopter with Suspended Load in Low Velocity Forward Flight

by

José J. Serpas Sigüenza

A THESIS

SUBMITTED TO THE FACULTY OF GRADUATE STUDIES

IN PARTIAL FULFILMENT OF THE REQUIREMENTS FOR THE

DEGREE OF MASTER OF SCIENCE

DEPARTMENT OF MECHANICAL AND MANUFACTURING ENGINEERING

CALGARY, ALBERTA

JULY, 2013

Abstract

A helicopter's vertical takeoff and landing, as well as its ability to hover, make it ideal for carrying a suspended load, which facilitates multiple military and civil applications in places of difficult access. The suspended load; however, alters the flight characteristics and degrades the handling qualities of the helicopter, which can lead to instability or a serious accident. This work proposes a controller for a helicopter slung load system in low velocity forward fight. The controller uses explicit model following with command generator tracker to adhere to the Aeronautical Design Standard 33 specified level 1 handling qualities. A load stability control (LSC) term is added to dampen load oscillation. Simulations show that the addition of the LSC term improves the system behaviour by damping load oscillation. Results also show that the LSC has little effect on the desired helicopter response with only a small deviation from the target behaviour.

Acknowledgements

I would like to acknowledge my supervisor Dr. Jeff K Pieper for his continuous support and guidance. It is because of this insight, advice and patience that I am able to complete this project.

I would also like thank my parents for their continuous and unquestioned support, not only while completing this project, but during my entire life. You have always inspired me to follow my dreams.

Finally, I would like to thank all of my friends and family who have helped me get to where I am today.

Table of Contents

List of Figures

Chapter 1 Introduction

1.1 Motivation

A helicopter's ability to perform vertical takeoff and landing, as well as hover, make it ideal for carrying and delivering a suspended load. This flight arrangement facilitates multiple military and civil applications including cargo transport in places of difficult access. One of its most common applications is for emergency response, allowing access to dangerous and otherwise nearly inaccessible environments; this includes firefighting and emergency sea rescue. In the private sector, it is particularly useful for the logging industry, where the timber is transported from the cut site to places of easier reach by trucks or trains. The use of helicopters removes the need for construction of roads that can be expensive and damaging to the environment. It is also useful for other industries like construction (Construction Helicopters Incorporated, 2008), oil and gas (Canadian Air-Crane Ltd, 2012), mining (Canadian Air-Crane Ltd, 2012) and maintenance of electric power lines (Parny, 1993).

The suspended load; however, alters the flight characteristics and degrades the handling qualities of the helicopter, which can cause an accident and lead to serious injuries or even death (Helicopter External Load Operations, 2006)(Cheetham & Buckingham, 1998). The problem is aggravated during high speed flight. Due to this, limits are imposed on the allowed forward velocity to less than half of the helicopter

design cruising flight speed (Isaev & Sumovskii, 1997), making it expensive in terms of both money and time.

The suspended load also increases the workload of the pilot, who not only has to control the helicopter but has to do it in a manner that results in minimum load oscillations. The pendulous motion of the load results in oscillations which can be aggravated by an inexperienced or distracted pilot trying to correct the motion. Making things worse is the lack of direct visual contact with the load by the pilot. Studies show that in more than half of accidents of slung load helicopter usage, human error is a factor (Shaughnessy & Pardue, 1977)(Veillette, 1999). The reduction of pilot workload by decreasing the need for corrective action would have positive effects in accident reduction.

1.2 Previous work

Because of its usefulness, research has been conducted to develop a stabilization system for a helicopter with a suspended load to assist the pilot by continuously attempting to reduce the load oscillations. There are three different proposed schemes: different slung load configurations, application of control action to the load itself and application of control action through helicopter movement.

The most commonly used configuration is known as single point suspension and is where the slung load is connected to the helicopter at a single point, Figure 1-1 (1-2).

This is also the most unstable configuration because there is no restriction to yaw motion of the load. At high velocities the yaw motion, depending on the load aerodynamics, can lead to undesired longitudinal and lateral movement of the load (Helicopter External Load Operations, 2006). Other configurations that use multiple suspension points, Figure 1-1 (3-5), give the pilot more control; however, there is a small amount of helicopters equipped with dual or multiple hook systems (Multiservice Helicopter Sling Load: Basic Operations and Equipment, 1997).

Stabilization can also be obtained by applying a control mechanism to the load itself by either modifying its aerodynamics or applying a control action. Modifying aerodynamics proposed schemes includes attaching controllable fins (Gera & Farmer, 1974)(Cicolani & Ehlers, Modeling and Simulation of a Helicopter Slung Load Stabilization Device, 2002) or a rudder to the load and placing a baffle in front of the load (Isaev & Sumovskii, 1997). For corrective action, proposed schemes include the use of jet propellers (Pardue & Shaughnessy, 1979), an active winch control system (Asseo & Sabi, 1971) and an active arms control system (Smith, Allen, & Vensel, 1973).

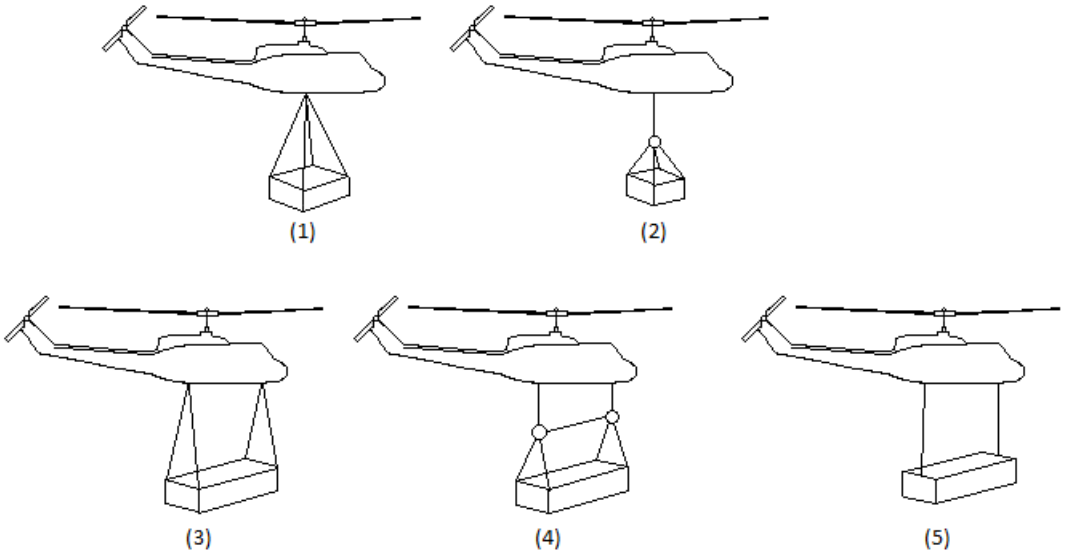

Figure 1-1 Examples of slung-load systems

Open Loop Control

There are two strategies used to control helicopter movements to reduce load oscillations: open loop shaping and closed loop or feedback control. Open loop control consist having the helicopter follow a predetermined trajectory which is defined to prevent oscillations from taking place. The main advantage of using this type of strategy is that there is no need to measure the system states. The most commonly used open loop technique to reduce vibrations and oscillations is input shaping.

Input shaping consists in dividing the input command into smaller commands that don't cause pendulations. This creates a staircase-like command, which is incremented by a small amount, held for a brief period of time and then incremented again. The process is repeated until the command signal matches the input reference signal. This technique is

simple to implement as it only requires an approximate value of the load swing frequency and damping ratio. The disadvantages of using this technique include that it cannot dampen pendulations from external disturbances and it introduces a small delay due to the filtering process involved.

This technique has been used to control load swing in cranes for some time. (Alsop, Forster, & Holmes, 1965) were the first to incorporate input shaping for gantry cranes when they proposed a two step acceleration/deceleration period to reduce load oscillation. They used an iterative procedure to define the acceleration/deceleration profile. (Hazlerigg, 1972) later proposed symmetric two-step acceleration deceleration profile. (Kuntze & Strobel, 1975) extended this research by introducing one or more zero-acceleration steps in the acceleration/deceleration profile. (Yamada, Fujikawa, & Matsumoto, Suboptimal control of the roof crane by using the microcomputer, 1983) proposed an acceleration profile based on Pontryagin's maximum principal, which minimized travel time while reducing load oscillations. (Jones & Petterson, 1988) and (Dadone & VanLandingham, 2001) used non-linear approximations and found improvement over linear approximations. (Garrido, Abderrahim, Gimenez, & Balaguer, 2008) proposed a two-part control system, the first was a basic input shaper to prevent swing as result of crane movement and the second was feedback control to eliminate external disturbances. (Ahmad, Ramli, Raja Ismail, Samin, & Zawawi, 2010) combined input shaping with a collated PD controller to reduce swing in a lab scale rotary crane. (Thalapil, 2012) proposed a method to optimized a robust input shaper.

Although input shaping has been used in cranes for some time, it has only recently been employed for helicopter slung load systems. (Bisgaard, 2008) was the first to apply this technique to an unmanned helicopter used for land mine detection. He proposed the use of an inner loop to control helicopter movement and an outer loop for load stability. He used a combination of feedforward control system based on input shaping for the helicopter and an optimized delayed feedback controller for load oscillation damping.

(Ottander & Johnson, 2010) combined input shaper with feedback control of the load swing angle. The proposed controller used input shaping to dampen load oscillations as result of helicopter motion and feedback control to dampen load oscillations as result of external disturbances.

(Potter, Singhose, & Costello, 2011) studied the effectiveness of applying different types of shapers to underslung helicopter loads. They tested a unity magnitude-zero vibration (UM-ZV) shaper which provides a faster response than the one proposed by Bisgaard. They also tested an extra insensitive (EI) shaper which provides more robustness to errors in the estimated natural frequency. They determined that the more robust controllers provide good results to model uncertainties while showing a small increase in travel time. The faster shaper was not as effective when dealing with model errors; however, still provided a significant improvement to an unshaped command.

(Adams, 2012) continued the work by Potter. He created a new modelling method to include the coupling between the helicopter and the load. The new model shows how the load affects the helicopter, which was no considered by Potter. Once the modeling was complete, Adams combined the input shaper design with model following control and tested it on an autonomous unmanned helicopter with promising results.

Feedback Control

The other strategy used to control helicopter movements to reduce load oscillations is state feedback design, in which the states are fed back to the controller where appropriate action is calculated and applied. A special type of feedback controller is optimal control, such as the linear Quadratic Regulator (LQR) where the states are multiplied by a constant and used as the system input without the use of a reference signal. The main advantage of using optimal control is that it provides corrective action with minimum control power usage.

(Vaha & Marttinen, 1989) used a combination of open loop control with feedback control. They employed the acceleration profile proposed by (Yamada, Fujikawa, & Matsumoto, Suboptimal control of the roof crane by using the microcomputer, 1983) and switched to a LQR when the trolley approached the target position to eliminate residual oscillations. (Abdul Kadir, Abd Wahab, Tomari, Shoiat@Ishak, & Hashim, 2009) used LQR theory to find the optimal parameter for a PID controller in order to reduce travel time in a Jib crane. (Zawawi, Wan Zamani, Ahmad, Saealal, & Samin, 2011) tested a PD

controller, a delayed feedback system and an LQR controller for a gantry crane and found that the LQR provides better performance in overshoot and settling time. Other researchers have combined LQR theory with other types of controllers like fuzzy (Adeli, M.; Zarabadipour, H.; Aliyari Shoorehdeli, M., 2011) and neural networks (Mendez, Acosta, Moreno, Hamilton, & Marichal, 1998), (Burananda, Ngamwiwit, Panaudomsup, Benjanarasuth, & Komine, 2002)

To stabilize loads suspended from a helicopter, optimal control has been considered, with a large part of the research focused on a hovering rotorcraft. (Gupta & Bryson, 1973) suggested a Linear Quadratic Regulator (LQR) controller for an S-61 Sikorsky helicopter for near hover stabilization with a single wire suspension. (Tsitsilonis & McLean, 1981) propose a solution to the numerical problems that resulted from the use of LQR controllers proposed by Gupta & Bryson. (Rachkov, Marques, & De Almeida, 2007) considered the stochastic disturbances acting at the load suspension point and reduced the load oscillation, as result the disturbances, thought optimum control with minimization of control power expenditure.

There are few cases of controller design for unmanned helicopters in flight. (Bernard, Kondak, & Hommel, 2008) developed an automatic control system which coordinates the movement of one or more helicopters for load transportation. The proposed controller uses an inner loop for robust control of the helicopter position and orientation, and an outer loop to stabilize the load by telling the helicopters how to move.

Although the LQR provides a little robustness to small modeling uncertainties, it is common to work with low order models which do not fully represent the system being modelled. In those cases a more robust controller may be needed to account for the unmodelled dynamics. One of the most commonly used robust controllers is H_∞, which considers the worst case or largest singular value. While this controller provides more robustness, it is also more difficult to obtain an optimal solution and in most cases a suboptimal controller is employed which affects the performance. (Faille & Van der Weiden, 1995) proposed the uses of H_∞ controller for robust regulation of a helicopter when a nacelle is hung from it by slings and the nacelle is either free or connected to an electrical high voltage line.

Fuzzy logic controllers are a more user friendly design technique, as they have the ability to work with imprecise or vague inputs known as fuzzy sets. Unlike classical or digital logic problems that use true/false, on/off or 1/0, fuzzy sets allow for intermediate discrete values of truth; which are defined with linguistic definitions rather than mathematical equations. Depending on the input and fuzzy values, an appropriate output is calculated through the use of if-then statements. The main advantage of working with fuzzy controls is that the controller can work with low resolution sensors and models, avoiding the need for highly detailed models and expensive sensors. This type of controller, however, can be difficult to tune as the control laws are defined on empirical experience and often require expert knowledge of the system.

(Yasunobu & Hasegawa, 1986) were the first to propose fuzzy control for a crane system. They used predictive fuzzy control by breaking crane operation into seven stages based on simplified trolley and load motions. (Yamada, Fujikawa, Takeuchi, & Wakasugi, 1989) proposed a fuzzy controller that imitated the acceleration profile used for input shaping by (Yamada, Fujikawa, & Matsumoto, Suboptimal control of the roof crane by using the microcomputer, 1983). They compared the fuzzy controller to input shaping and found that it provides better disturbance rejection. (Kim & Kang, 1993) used two models to determine trolley and cable velocities and used two fuzzy controller to track those velocities. (Itoh, Migita, Itoh, & Irie, 1993) used fuzzy control strategy to imitate an input shaping acceleration profile. Simulation results show that this controller is more effective than input shaping and skilled operators. (Moustafa, Ismail, Gad, & El-Moneer, 2006) proposed a fuzzy control system that considers flexible and time-dependant cable lengths. (Ahmad, Samin, & Zawawi, Comparison of Optimal and Intelligent Sway Control for a Lab-Scale Rotary Crane System, 2010) studied the use of PD-fuzzy controller and found that they provide better performance than traditional optimal control. (Abdullah, Ruslee, & Jalani, 2011) compared fuzzy controllers to conventional LQR and found that they reach the desired oscillations-free position in similar amounts of time but with smaller maximum swing values.

(Omar, 2009) proposed a fuzzy based anti-swing controller for a helicopter slung load system near hover flight. The controller is divided into two parts: trajectory tracking and anti-swing. The anti-wing output is an additional displacement in horizontal and

lateral directions, which are added to the helicopter desired trajectory. The anti-swing law design is based on time-delayed feedback of the load swing angles.

Newer control techniques include adaptive controls such as neural networks. A neural network controller works like a brain that "learns" as it gains experience. This means that they have the ability to adapt and modify the system model or control laws depending on previous experience. The main issue with neural networks is that they may require extensive and diverse training in order to be used for real-world applications.

(Mendez, Acosta, Moreno, Hamilton, & Marichal, 1998) proposed a combination of neural networks with optimal control to reduce load oscillation in an overhead crane system. The proposed controller used a state feedback controller for crane movements and an on-line neural networks system to learn about the crane dynamics. The on-line neural network is then used to self-tune the state feedback controller. (Burananda, Ngamwiwit, Panaudomsup, Benjanarasuth, & Komine, 2002) proposed a similar combination of state feedback controller and neural networks. They used an LQR design with typical LQR control methods. An on-line neural network is then used to modify the LQR gains and improve performance. (Chih-Hui & Chun-Hsien, 2010), proposed the use of a model-less adaptive output recurrent neural network for crane control (AORNN). They used an analytical method based on Lyapunov functions to determine the learning-rates of AORNN and guarantee stability.

In helicopter applications, company called Neural Robotics developed and autonomous aerial vehicle that was reported to be able to handle gusting winds without any problem (Crane, 2006) and even released a video demonstration (AutoCopter, 2011). The Autocopter as it is known, uses a neural network algorithm that allows the user to fly the rotorcraft in two settings: semi-autonomous and fully autonomous. In the semi-autonomous settings, the user is in control and commands the helicopter how to move. In fully autonomous, the helicopter uses GPS system to follow a predetermined flight path.

1.3 Contribution

Controller

This thesis proposes a control system for a helicopter traveling with a slung load in low velocity forward flight (up to 45 knots), which assists the pilot by damping oscillations from the suspended load. The controller is not intended to replace the pilot and create an autonomous vehicle, but rather to assist the pilot to better control the rotorcraft by lessening the workload required to achieve the desired flight conditions. Other controllers have been created for autonomous helicopters that consist of two controllers; one that is used to achieve a desired helicopter attitude and velocities, and the other that tells the helicopter how to move by creating a set of commands needed for the helicopter to reach its desired position. While those controllers have shown promising results, autonomous vehicles offer limitations in unknown and changing environments (Siegwart & Nourbakhsh, 2004). For this type of environments, a human pilot has the

skills and judgement necessary to determine how the helicopter needs to move, and correct when necessary.

The proposed controller is designed to follow human generated commands, rather than create its own, to arrive at a given location. It is intended to be a stability augmentation system that makes corrections, when needed, to help the pilot control the suspended load. In instances where the pilot has good control with little load swinging, the controller will be required to do little; while in instances where large swinging occurs, the controller will have to make larger corrections to reduce the swing or help the pilot regain control of the helicopter. This is accomplished through the synthesis of a model following controller that mimics an ideal model derived from the ADS-33 (Aeronautical Design Standard, Performance Specification, Handling Qualities Requirements for Military Rotorcraft, 2000) specified level 1 handling qualities, which is reviewed in Section 2.5. A load stability control (LSC) term is then added to the controller to dampen load oscillation.

Simulation model

The simulation model presented in this thesis consists of the expansion of an existing helicopter model to include the suspended load. In cases where the helicopter model is known, it is useful to model the slung load system by expanding the original model, rather than creating a new one from scratch. The process is similar to that

presented in (Thanapalan & Wong, Modeling of a Helicopter with an Under-Slung Load System, 2010), but expanded to show the effect the load has on the helicopter.

1.4 Organization

This thesis is divided into 6 chapters of which this chapter is the first. Chapter 2 provides background related to how helicopters are able to remain aloft and how they are controlled. It briefly explains the concepts of lift and drag and how each of them affects the helicopter. Later, it describes the basic control mechanisms present in most helicopters, the challenges of piloting a helicopter and the type of augmentation needed to improve the handling qualities. The chapter also mentions the methods used to define the handling qualities and the minimum requirements needed to ensure satisfactory flight conditions.

Chapter 3 describes the process used to model the helicopter under-slung load system. The process consists of expanding an existing helicopter model to produce one for the under-slung system. This is achieved by first deriving the equations for the load, which is modelled as a pendulum with a mobile suspension point. After that, the cable tension is added to the helicopter and its effect analysed. The resulting expanded model represents the helicopter under-slung system.

Chapter 4 presents the design process used to synthesise a model following controller that attempts to copy an ideal model derived from the ADS-33 specified level 1

handling qualities. It first describes the Linear Quadratic Regulator (LQR) and analyses its properties to determine whether it can be used for this application. It then proceeds to describe a modified LQR design process so that the controller tries to reduce the error between the helicopter response and an ideal model, driving it to zero. The explicit model following (EMF) with command generator tracker technique (CGT) is presented as well as a load stability control (LSC) term.

Chapter 5 shows the simulation results of the application of the model following controller to a Bell 205 (UH-1H) helicopter. It shows that there is significant load oscillation damping when the LSC term is added to the controller. Results also show that the LSC has little effect on the desired helicopter response with only a small deviation from the target behaviour and good directional decoupling. Chapter 6 contains conclusions and suggestions for further research.

Chapter 2 Helicopter Flight Theory

2.1 Introduction

Helicopters are versatile vehicles with six degree of freedom motion. They use the same flight principles as airplanes of creating lift and drag. These phenomena are described in Sections 2.2 and 2.3 as they contain information that will be later used in Section 3.3. Section 2.4 describes the basic control mechanisms present in most helicopters, the challenges of piloting a helicopter and the type of augmentation needed to improve the handling qualities. Section 2.5 mentions the methods used to define the handling qualities and the minimum requirements needed to ensure satisfactory flight conditions.

2.2 Helicopter flight principles

Next is a brief explanation of the principles that allow helicopters to remain aloft and the controls used to manoeuvre the rotorcraft. There are several excellent textbooks in the area including those by (Seddon & Newman, 2002), (Balmford & Done, 2000), (Padfield, 2007) and (Wagtendonk, 2006).

2.2.1 Lift

Helicopters use the same principles as airplanes that enable them to fly. Helicopter need to generate an upward force to overcome the weight of the aircraft enabling it to keep aloft. This force is known as lift. Lift is a force generated by the interaction of the wing of the rotorcraft and the air surrounding it, which is deflected and results in a variation of atmospheric pressure around the surface of the wing. The difference between helicopters and airplanes is that planes have wings which are attached to the body and move with it while the helicopter has blades that rotate independently of the body, allowing it to perform manoeuvres like vertical takeoff and landing, lateral movement and hovering. The phenomenon of lift is described by Bernoulli's principle which can be stated as

Pressure energy + dynamic energy = constant (Wagtendonk, 2006)

This means that when there is an increase in a fluids speed, there is a simultaneous decrease in pressure, and vice versa. Wings have special designs that accelerate the air at the top of the wing, leading to a difference of pressure between the top and bottom, as seen in Figure 2-1. Because the lower part has a higher pressure than the top, the wing, and thus the aircraft, is pushed up, allowing it to remain aloft.

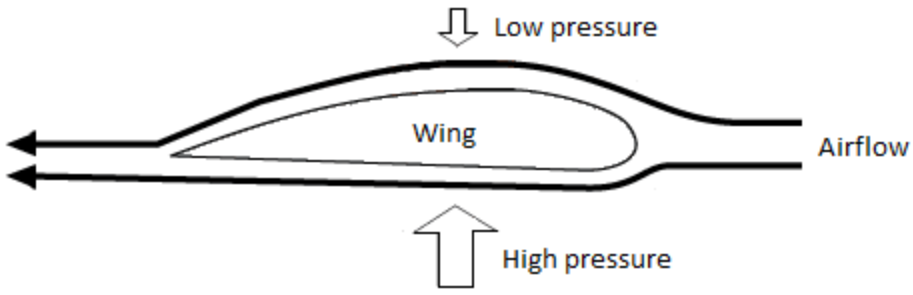

Figure 2-1 Lift generation

Lift is described by the formula

$$lift = \frac{1}{2} C_L \rho V^2 S \tag{2.1}$$

where

C_L = the lift coefficient

ρ = the density of the surrounding air

V = the airflow velocity of the surrounding air

S = the surface area perpendicular to the airflow direction

The lift coefficient depicts the ability of an object to deflect an airflow and depends on the shape and orientation of the object. The lift coefficient can be modified by changing the angle of attack, which is the angle created between the cord of the blade and the relative airflow, as seen in Figure 2-2. The cord is the straight line between the blade's leading edge and its trailing edge. Typically a larger angle of attack results in a larger lift

coefficient and a smaller angle results in a smaller lift coefficient. The variation is fairly linear for small angles until a maximum value is reached (Wagtendonk, 2006). The angle of attack where the maximum occurs is known as the critical angle of attack, and for angles larger than this the lift coefficient decreases.

Another way to modify the lift created is by varying the true air speed, that is, the speed at which the blade moves through the air. Because velocity is squared in the formula, changes in velocity result in larger changes in lift created. For helicopters, this velocity depends on the rotor angular velocity, as this determines the linear velocity of any point of the blade. Helicopters have fairly constant rotor angular velocity, so the lift variation due to velocity change is very small. This means that the main way to increase or decrease lift is to change the lift coefficient, which in turn means changing the angle of attack.

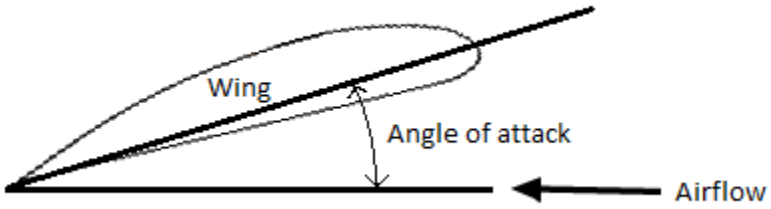

Figure 2-2 Angle of Attack

2.2.2 Drag

Drag is a force, similar to lift, that is created when an object moves through air, except that it acts as a resistance to the motion. The formula to describe drag is similar to that of lift

$$drag = \frac{1}{2} C_D \rho V^2 S \tag{2.2}$$

where

C_D = drag coefficient

The drag coefficient represents an object's potential to interfere with a flow of fluid (liquid or gas). Like the lift coefficient, it depends on the shape and orientation of the object. The drag is lowest when the angle of attack is zero degrees and increases as the angle of attack deviates from zero, regardless of direction.

The total drag that an aircraft experiences depends on different factors and is a combination of parasitic and induced drag.

2.2.3 Parasitic drag

Parasitic drag is created by any part of the aircraft that does not provide lift. In helicopters the blades are responsible for creating lift and everything else creates parasitic

drag, this includes the fuselage, landing gear and tail surfaces. The most important consideration of parasitic drag is that it varies with the velocity squared, so that when traveling at high speeds it can be very large. This type of drag becomes of great interest when traveling with objects attached to the outside of the cabin, such as slung loads. In these cases, the maximum payload for the helicopter may not be reached; however, because of the extra drag generated, the helicopter cannot perform at the same level as when the load is inside.

This type of drag can be divided into form drag and skin friction. Form drag is caused by the impact on the front and back surfaces of the object. Certain shapes can cut through an airflow easier than others; for example, a rounded surface has a much lower impact than a flat surface and a teardrop shape can reduce the turbulence formed at the rear. The shape of the object has a direct impact on the drag coefficient, so it is important to work with aerodynamic shapes in order to reduce drag. The drag coefficient for common shapes can be seen in Table 1 (Szuladzinski, 2009).

Table 1 Drag coefficients for common shapes

Drag Coefficient C_D for Common Shapes	
Object	**C_D**
Sphere	0.47
Cube, face-on	1.10
Cube, edge-on	0.80
Circular cylinder, side-on	0.75
Square cylinder, side-on	2.00
Square cylinder, long edge-on	1.60
Triangular, 60° cylinder, face-on	2.20
Triangular, 60° cylinder, edge-on	1.39
Long circular cylinder, side-on, laminar	1.20
Long circular cylinder, side-on, turbulent	0.30
Long circular cylinder, end-on	1.00
Long, thin plate, face-on	1.40
Long, thin plate, edge-on	1.50
Open hemisphere, concave against wind	1.40
Open hemisphere, convex against wind	0.40
Disk, face-on	1.10

Skin friction is created by the interaction of the object surface and the air moving around it. The air molecules next to the surface are almost stationary with respect to the object and increase in speed the further they move from the surface until they reach the speed of the airflow. The small layer between the surface and the free moving airflow is called the boundary layer and can be either laminar or turbulent.

2.2.4 Induced drag

Induced drag affects the blades and is the result of the downwash. As lift is generated, the passing air is pushed down, which influences the direction of the oncoming airflow and causes it to approach the leading edge from above. The rotor downwash is related to the lift generated and thus the angle of attack, the larger this

angles, the larger the downwash. The change in the airflow direction results in a change in the total reaction when the air is deflected.

2.3 Anti torque rotor

As was described in section 2.2, helicopters are able to fly because of the lift generated from the movement of the rotor blades. The spinning motion allows for lift to be created without the need to move the fuselage. One of the problems of working with a rotor to provide lift is that it creates a torque which tries to rotate the body of the helicopter in the opposite direction of the rotor. To prevent this motion, helicopters must employ an anti-torque mechanism which creates an equal but opposite torque. There are many mechanisms that achieve this, with the most common being the addition of a second rotor. Many helicopters use a small tail rotor, which works with the same principles as the main rotor, except it is placed vertically so that it creates sideways thrust, as seen in Figure 2-3. This rotor is directly connected to the main one and tends to "bleed off" power. Other solutions involve the use of two main rotors which rotate in the opposite directions. Configurations for this include tandem (non-overlapping), co-axial and intermeshing. Some helicopters use the NOTAR system which takes advantage of the Coandă effect and uses the main rotor downwash to cancel out the torque.

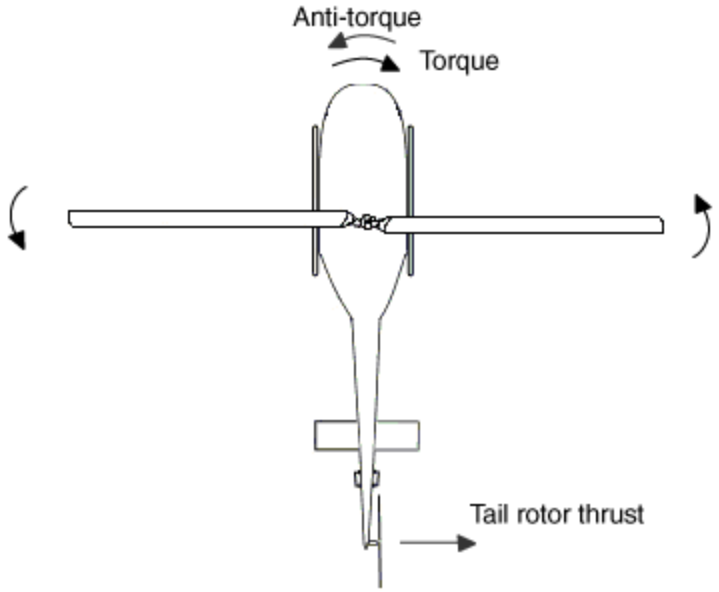

Figure 2-3 Anti-torque rotor

2.4 Helicopter controls

As was mentioned in section 2.2.1, the main rotor angular velocity remains constant so the only way to modify the lift generated is to change the angle of attack of the blades. To modify the angle of attack of all the blades at once, helicopters use a mechanism similar to the one shown in Figure 2-4, known as a swashplate. The swashplate arrangement consists of two circular plates positioned one on top of the other. The bottom plate is fixed to the fuselage while the top one rotates along with the rotor; rollers are used to allow movement between the plates. The top plate is also connected to the individual blades through pitch links which are fitted to either the leading or trailing edge of the blade. The plates are connected in a manner that forces them to always be parallel to each other and thus the top one must replicate the motion of the bottom one.

Control of the helicopter is achieved by moving the bottom plate up and down or tilting it. There are four control inputs the pilot uses to maneuver the helicopter: the main rotor collective, the longitudinal cyclic, the lateral cyclic and the tail rotor collective.

Collective control consists in sliding the plates up or down to modify the angle of attack of all the blades equally, Figure 2-5 top. When the attack angle is increased all the blades generate more lift and likewise, when the attack angle is decrease all blades generate less lift. The result is a variation of the total thrust without altering its orientation, leading to vertical displacement. The tail rotor collective works in the exact same manner but applied to the tail rotor instead of the main rotor. Because of the tail rotor placement and function, a variation of this control results in yaw motion of the helicopter.

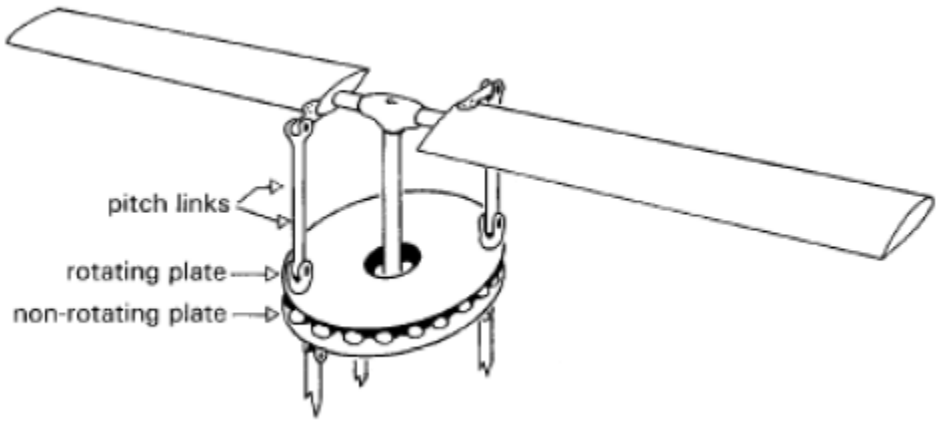

Figure 2-4 Helicopter control swashplate[1]

[1] Image source: G. D. Padfield, *Helicopter Flight dynamics*, 2nd ed. Blackwell Publishing, 2007

Cyclic control consists in the tilting of the plates rather than a sliding motion. This action increases the attack angle of the blades in one side and reduces it in the blades of the opposite side, Figure 2-5 bottom. As a result, the thrust generated on side of the aircraft is larger than the one generated on the opposite side, leading to a change in orientation of the total thrust. Cyclic control is often divided into longitudinal and lateral depending on the desired flight direction. Longitudinal control tilts the plate in the pitch axis, resulting pitch action and lateral csontrol tilts it in roll axis, resulting in roll action.

A strong relation is present among the axes and the application of a specific control action, with the intention of motion in a specific axis, can lead to undesired movement in another axis. For example, increasing anti-torque to rotate the helicopter about the yaw axis increases the power demands of the tail rotor, which in turn bleeds off power from the main rotor. Unless more power is applied, the helicopter rpm will decrease and the helicopter will begin to descend. Likewise, if anti-torque control is decreased, the helicopter will tend to ascend unless the main rotor power is reduced accordingly. This relation is known as coupling and is more pronounced for the vertical-yaw and pitch-roll axes. Because of coupling, simultaneous application of multiple control inputs is necessary to perform a desired maneuver.

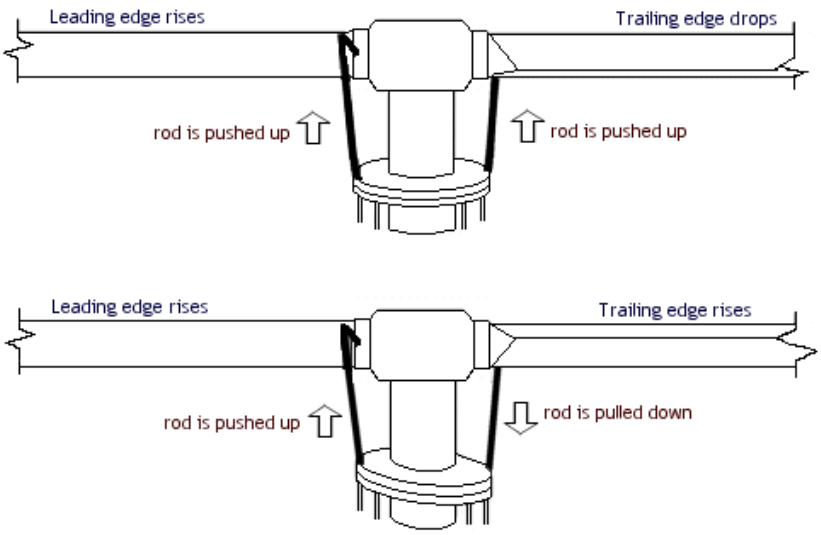

Figure 2-5 Top: collective control. Bottom: cyclic control

2.5 Handling Qualities Requirements

To ensure the helicopter behaviour, minimum handling qualities specifications are defined. The handling qualities describe how easy it is for the pilot to accomplish a desired task while maintaining control of the rotorcraft. The handling qualities of a helicopter describe how easy it is for the pilot to accomplish a desired task while maintaining control of the rotorcraft. During the 1980s, this topic became of interest to the United States Army and other agencies, which began to reconsider previous handling qualities specifications in military helicopters seeking to reduce the pilot workload. Because of this, new standards were developed and the Aeronautical Design Standard 33 (ADS-33) (Aeronautical Design Standard, Performance Specification, Handling Qualities Requirements for Military Rotorcraft, 2000) was introduced. The ADS-33 defines the minimum requirements of acceptable handling qualities in order to assure that any

deficiencies will not compromise the flight safety or the capability of completing the given mission.

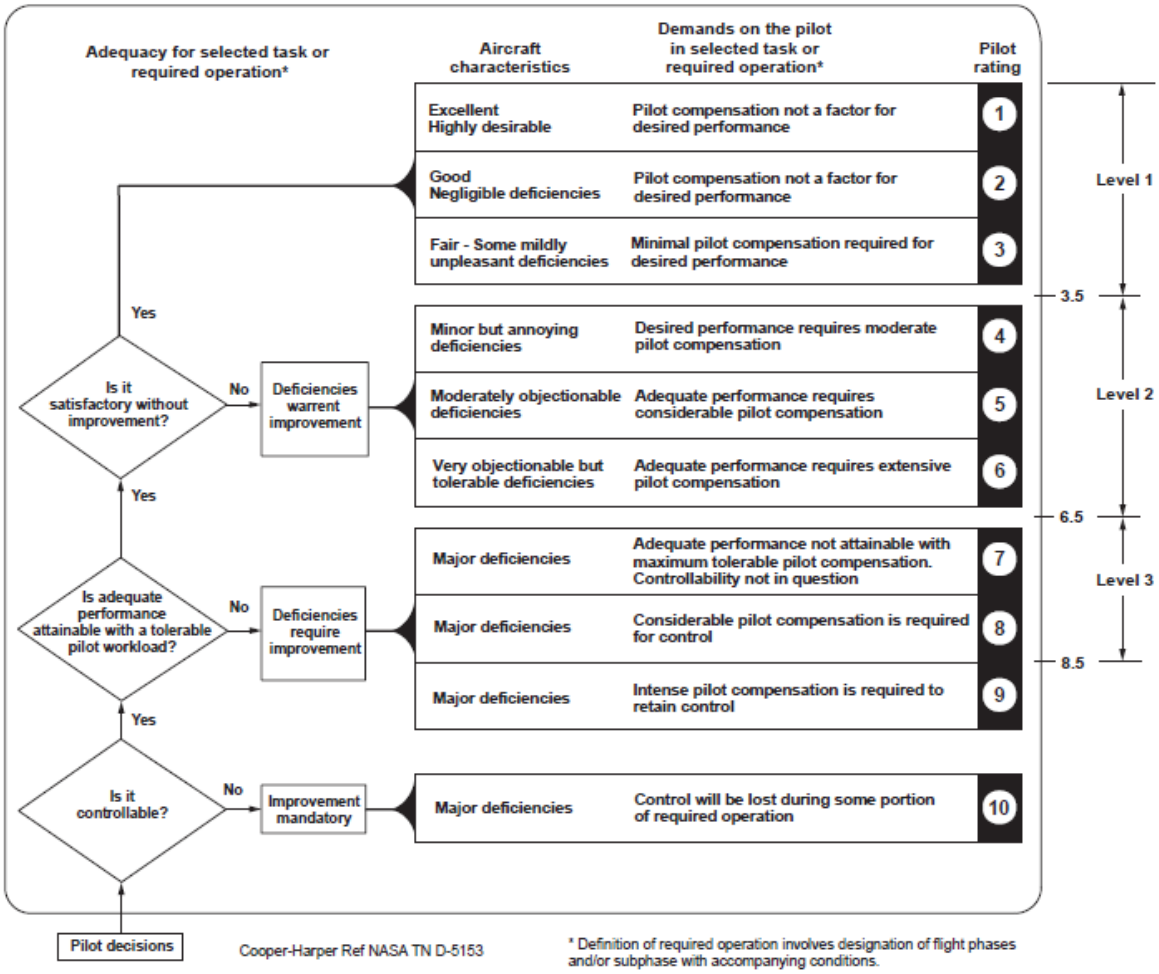

Figure 2-6 Cooper-Harper rating scale[2]

The handling qualities are classified using the Cooper-Harper handling qualities rating (Cooper & Harper Jr., 1969), Figure 2-6, which ranges from one to ten. A rating of one represents the ideal flight conditions and ten represents uncontrollable conditions.

[2] Image source: "Aeronautical Design Standard, Performance Specification, Handling Qualities Requirements for Military Rotorcraft," United States Army Aviation and ADS-33E-PRF, 2000

The Cooper- Harper rating scale is further divided into three levels to define a range of acceptable handling qualities. Level 1 is the ideal or desired level of flight, level 2 is acceptable but undesired, and level 3 is unacceptable.

2.5.1 Response type

Different situations require different control methods in order to allow the pilot to maintain both control and stability of the aircraft. Because of this, multiple control configurations, called response types, have been created to provide different responses to a given pilot command. Response types define how much control is in the hands of the pilot and how much depends on a computer control system.

The required response type for different flight conditions depends on the Mission-Task- Elements (MTE) and the Usable Cue Environment (UCE), which describe the task that the pilot is required to do and the environmental conditions where flight will take place. The UCE range from 1 to 3, where 1 is normal daylight visual environment and 3 is extremely poor visual environment. Normally, in good flight conditions (UCE 1) Rate Command will be sufficient to accomplish level 1 flight for most tasks, as it is very flexible for manoeuvring. Rate Command refers to instances when the helicopter responds with angular rate behaviour, in a specific axis, when a step input is given by the pilot in that axis. For adverse conditions (UCE 2), more dependence on control systems is needed and other response types, such as Attitude Hold, are required. Attitude Hold implies that the aircraft will maintain the current angular attitudes in all axes when zero

pilot commands are given. This response type is also recommended for performing most tasks during hover or low speed flight.

Next is a list of the different response types:

- Rate Command Attitude Hold (RCAH): Stick command actuation is proportional to angular rate for aircraft. Null command results in constant attitude and heading, that is zero rate.
- Rate Command/Direction [Heading] Hold (RCDH) : Null command implying zero rate in heading change
- Rate Command/Height [Altitude] Hold (RCHH): Vertical direction (collective input) rate command response with null input implying hold of altitude. Null command implying zero rate in altitude change.
- Position Hold (PH): The rotorcraft automatically holds its position with respect to a ground fixed or shipboard hover reference.
- Attitude Command/Attitude Hold (ACAH): Stick command is proportional to attitude or heading changes for aircraft. Null commands result in returning to zero degree attitude.
- Translational Rate Command (TRC): Rate command inputs in lateral and forward velocity directions. Translational rates are commanded directly.

The rank-ordering of combinations of Response-Types from least to most stabilization is defined as:

1. RATE (all axes)
2. RATE+RCDH+RCHH+PH
3. ACAH+RCDH
4. ACAH+RCDH+RCHH
5. ACAH+RCDH+RCHH+PH
6. TRC+RCDH+RCHH+PH

For acceleration and deceleration (depart/abort) in a UCE 2, ADS-33 calls for Attitude Command/Attitude Hold (ACAH) response in pitch and roll axes, Rate Command/Height Hold (RCHH) response in vertical axis and Rate Command/Direction Hold (RCDH) response in yaw axis. These are defined as the minimum stability requirements. A specified response type may be replaced with a higher rank of stabilization

2.5.2 Bandwidth and Phase Delay

Depending on the magnitude of change of the fight configuration, helicopter manoeuvres are classified into three different classes which are small amplitude, moderate amplitude and large amplitude. Special attention is paid to small amplitude manoeuvres because it is desired that the rotorcraft be insensitive to external disturbances; thus, allowing precise manoeuvring. Two common parameters used to measure the helicopter performance are the system bandwidth and phase delay margin, which measure the time delay from control input to attitude response. If there is a large

time delay, as result of limited bandwidth gain and large phase delays, then there is the possibility for pilot induced oscillation.

Bandwidth is defined as either the frequency at which the system gain is 6dB higher than the system gain at which the system exhibits a lag of -180 degrees ($\omega_{BW_{gain}}$) or the frequency at which the phase is -135 degrees ($\omega_{BW_{phase}}$). The required bandwidth depends on the response type in use. For ACAH response the bandwidth will be $\omega_{BW_{phase}}$. For Rate response types, the bandwidth will be whichever one is lower between $\omega_{BW_{gain}}$ and $\omega_{BW_{phase}}$.

The phase delay is defined as the ratio of system phase lag exceeding -180 degrees at twice the frequency where -180 degrees phase lag was first observed, measured in radians, divided by this frequency

$$\tau_p = \frac{\Phi - \pi}{2\omega_{180}} \tag{2.3}$$

where

$2\omega_{180}$ = twice the frequency where -180 degrees phase lag was first observed

Φ = the phase lag at $2\omega_{180}$ in radians

When working with phase lag in degrees, the phase delay can be expressed as

$$\tau_p = \frac{\Phi - 180}{57.3(2\omega_{180})}$$

2.5.3 Time Constant

Moderate amplitude manoeuvres are typically measured for performance by minimum requirements in the equivalent transient time constant for this axis. That is the parameter τ_r that roughly satisfies the differential equation

$$\tau_r \dot{x} = -x + u_x \tag{2.4}$$

In some axis x, for the input driving function u_x. This parameter is, for practical purposes measured as the ratio

$$\tau_r = \frac{q_{peak}}{\Delta\theta_{peak}} \tag{2.5}$$

where

q_{peak} = the maximum magnitude or peak value of pitch angular rate during the manoeuvre

$\Delta\theta_{peak}$= the total attitude pitch change during the manoeuvre

Equation 2.5, is an example using the pitch axis. It can also be used for motion in the other axes.

2.5.4 Detailed handling qualities specifications pitch and roll axes

The following specifications are based on the ADS-33 (Aeronautical Design Standard, Performance Specification, Handling Qualities Requirements for Military Rotorcraft, 2000) requirements for level 1 flight while in low velocity flight and hover. Low velocity flight is defined as that which is lower than 45 knots.

For small amplitude attitude changes, a bandwidth of 3.0 rad/s and a phase delay of 0.2 s will suffice to obtain level 1 flight for most manoeuvres. The lone exception is target acquisition and tracking where a bandwidth of 4.0 rad/s and a phase delay of 0.1s are required. This works as long as any oscillatory modes following an abrupt controller input have an effective damping ratio of at least $\zeta = 0.35$.

For moderate attitude changes, the ratio of peak pitch (roll) rate to change in pitch (roll) attitude, (τ_r), shall be of at least 1.0 s^{-1} for pitch and 1.5 s^{-1} for roll for most manoeuvres. For Target Acquisition and Tracking, the requirements are much higher. The cross-coupling ratio between the pitch and roll axes shall not be greater than ±0.25.

This means that a variation in pitch attitude $\Delta\theta$ is not allowed to produce a variation in the roll attitude $\Delta\varphi$ of more than 0.25 $\Delta\theta$, and vice versa.

2.5.5 Detailed handling qualities specifications yaw and vertical axes

The following specifications are based on the ADS-33 (Aeronautical Design Standard, Performance Specification, Handling Qualities Requirements for Military Rotorcraft, 2000) requirements for level 1 flight while in low velocity flight and hover. Low velocity flight is defined as that which is lower than 45 knots. For small amplitude attitude changes a bandwidth of 3.0 rad/s and a phase delay of 0.2 s will suffice to obtain level 1 flight for most manoeuvres. The lone exception is target acquisition and tracking where a bandwidth of 4.0 rad/s and a phase delay of 0.2s are required. This works as long as any oscillatory modes following an abrupt controller input have an effective damping ratio of at least $\zeta = 0.35$.

For moderate attitude changes, the ratio of peak yaw rate to change in yaw attitude, (τ_r), shall be of at least 1.5 s^{-1} for most manoeuvres. For Target Acquisition and Tracking, the requirements are much higher. The cross-coupling ratio between the yaw and vertical axes is to meet the following specifications for level 1 flight. The maximum magnitude of the ratio of maximum yaw rate experienced before 3 seconds divided by the vertical translation rate achieved after 3 seconds shall be kept lower than 0.65 deg/s/ft/s. The maximum magnitude of the ratio of yaw rate experienced after 3 seconds divided by the vertical translation rate achieved after 3 seconds shall be kept lower than 0.15 deg/s/ft/s.

Pitch and roll attitudes shall be maintained essentially constant. In addition, there shall be no objectionable yaw oscillations following step or ramp collective changes in the positive and negative directions. Oscillations involving yaw rates greater than 5 deg/sec shall be deemed objectionable.

Chapter 3 Slung Load System Modelling

3.1 Introduction

The slung load system modelling consists of expanding an existing helicopter model to produce one for the under-slung system. This is achieved by first deriving the equations for the load, which is modelled as a pendulum with a mobile suspension point. After that, the cable tension is added to the helicopter and its effect analysed. The resulting expanded model represents the helicopter under-slung system. The process is similar to that presented in (Thanapalan & Wong, Modeling of a Helicopter with an Under-Slung Load System, 2010), but expanded to show the effect the load has on the helicopter.

3.2 Helicopter model

Helicopters often have teetering rotors and move as result of a complex process involving cockpit stick dynamics, actuator dynamics, rotor tip path plane dynamics and body motion, producing high-order models. These high-order models are tough to use and often reduced to low-order in order to make them more manageable to work with. Even though low-order models do not fully represent helicopter dynamics, they are commonly used for controller design as they provide an acceptable approximation and simplify the design and implementation process.

Helicopter dynamics are also non-linear; however, many design techniques can only be applied to linear systems and thus linear approximations are calculated for a variety of trim conditions. With possible variations of the states order, a low order linear helicopter model has the following structure

$$\dot{x} = Ax + Bu$$

where

$$x = \begin{bmatrix} U \\ W \\ Q \\ V \\ P \\ R \\ \theta \\ \phi \end{bmatrix} = \begin{bmatrix} forward\ velocity \\ vertical\ velocity \\ pitch\ rate \\ lateral\ velocity \\ roll\ rate \\ yaw\ rate \\ pitch\ attitude \\ roll\ attitude \end{bmatrix}$$

$$u = \begin{bmatrix} \delta_C \\ \delta_B \\ \delta_A \\ \delta_P \end{bmatrix} = \begin{bmatrix} collective \\ longitudinal\ cyclic \\ lateral\ cyclic \\ tail\ rotor\ collective \end{bmatrix}$$

The values of A and B are obtained for specific helicopters and operating conditions through methods like published documents (Heffley, Jewell, Lehman, & Van Winkle, 1979)(Stuckey, 2001), directly from the manufacturer, or direct derivation (Padfield, 2007) (Thanapalan, Modelling of A Helicopter System, 2010). An example is the linear low-order model for a Bell 205 helicopter in hover is described by:

$$A = \begin{bmatrix} 0 & 0.03 & 0.18 & -0.01 & -0.42 & -0.08 & -9.81 & 0 \\ -0.10 & -0.39 & 0.09 & -0.10 & -0.12 & 0.68 & 0 & 0 \\ 0.01 & -0.01 & 0.09 & 0 & 0.23 & 0.04 & 0 & 0 \\ 0.02 & 0 & -0.41 & -0.05 & -0.27 & 0 & 0 & 9.81 \\ 0.03 & -0.02 & -0.88 & -0.04 & -0.57 & 0.14 & 0 & 0 \\ -0.01 & -0.02 & -0.06 & 0.07 & -0.32 & -0.71 & 0 & 0 \\ 0 & 0 & 1 & 0 & 0 & 0 & 0 & 0 \\ 0 & 0 & 0 & 0 & 1 & 0 & 0 & 0 \end{bmatrix}$$

$$B = \begin{bmatrix} 0.08 & 0.13 & 0 & 0 \\ -1.17 & 0.04 & 0 & 0.01 \\ 0 & -0.07 & 0 & 0.01 \\ -0.04 & 0 & 0.11 & 0.20 \\ -0.04 & 0 & 0.22 & 0.17 \\ 0.17 & 0 & 0.03 & -0.47 \\ 0 & 0 & 0 & 0 \\ 0 & 0 & 0 & 0 \end{bmatrix}$$

The angular rates are measured in rad/s, translational rates in m/s and angular attitudes in rad. The control inputs are in terms of pilot stick movement, measured in cm.

3.3 Under-slung load model

The main objective of the study is to analyze the load motion during helicopter acceleration and stopping. For this reason, a two dimensional model is used as it will suffice to show the longitudinal displacement of the load. The load is considered to be single point suspension, subjected only to drag forces, weight and cable tension, as presented in (Thanapalan & Wong, Modeling of a Helicopter with an Under-Slung Load System, 2010) and illustrated in Figure 3-3. No aerodynamic properties are considered aside from the drag forces, which are proportional to the square of the velocities and always oppose the direction of motion. The rotor downwash effects are neglected. The

cable is considered rigid, massless, and with no aerodynamic properties. Despite these limitations, the system has proven adequate for simulation studies in which the low-frequency behaviour is of primary interest and the helicopter is initially trimmed in forward flight (Cicolani, Kanning, & Synnestvedt, Simulation of the dynamics of helicopter slung load systems, 1995). To facilitate combining the models, the slung-load equations are derived using the helicopter reference coordinates as illustrated in Figure 3-2. It is also assumed that the velocity of the suspension point is the same as that of the helicopter center of gravity.

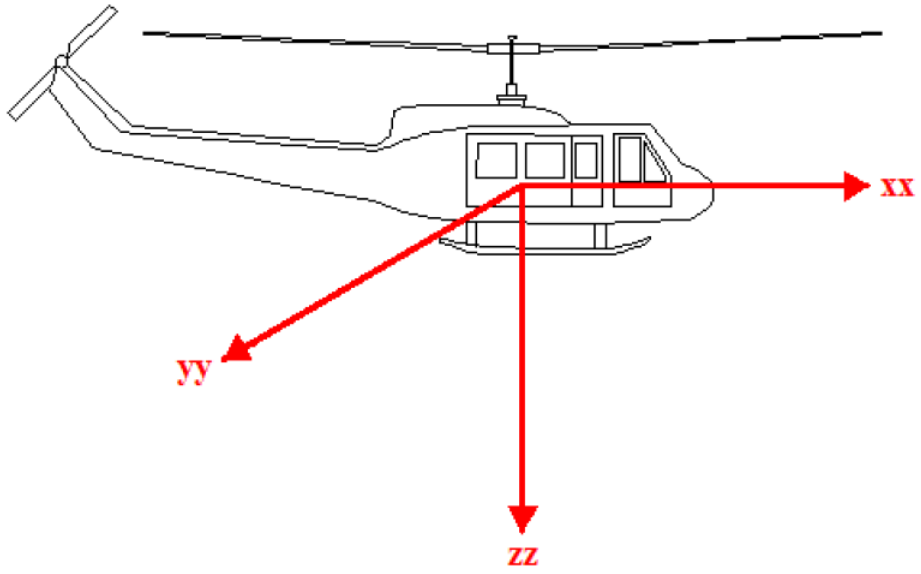

Figure 3-1 Helicopter reference frame

where

xx= the helicopter longitudinal axis

yy= the helicopter lateral axis

zz= the helicopter vertical axis

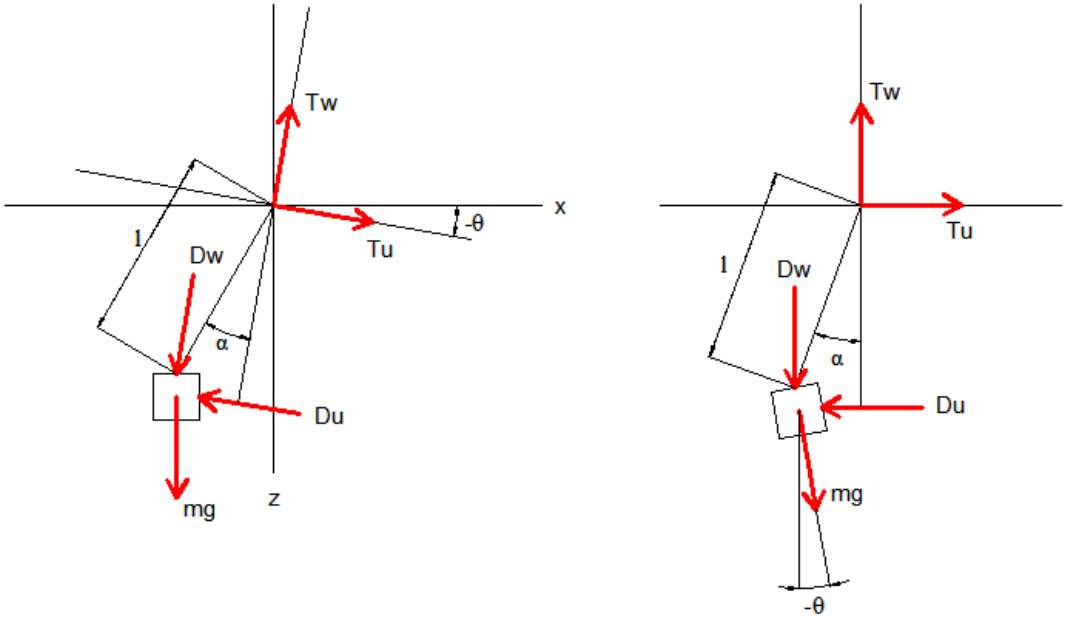

Figure 3-2 Under-slung load system

From first principles derivation and geometry as per Figure 3-2, it is possible to calculate

$$U_L = U - lcos\alpha\dot{\alpha} \tag{3.1}$$

$$W_L = W - lsin\alpha\dot{\alpha} \tag{3.2}$$

$$D_U = C_U sign(U_L){U_L}^2 \tag{3.3}$$

$$D_W = C_W sign(W_L){W_L}^2 \tag{3.4}$$

And differentiating

$$\dot{U}_L = \dot{U} - l(cos\alpha\ddot{\alpha} - sin\alpha\dot{\alpha}^2) \tag{3.5}$$

$$\dot{W}_L = \dot{W} - l(sin\alpha\ddot{\alpha} + cos\alpha\dot{\alpha}^2) \tag{3.6}$$

where

α = the angle between the helicopter vertical axis and the load (load angle)

U_L= the load longitudinal velocity

W_L= the load vertical velocity

D_U= the drag force as result of longitudinal movement

D_W= the drag force as result of vertical movement

T_U= the cable tension in longitudinal axis

T_W= the cable tension in vertical axis

U, W = the helicopter longitudinal and vertical velocity, as previously defined

Moments about suspension point gives

$$I_{ysp}\ddot{\alpha} = D_U l cos\alpha - D_W l sin\alpha - \big(mgcos(\theta)\big)(lsin\alpha) - \big(mgsin(\theta)\big)(lcos\alpha)$$

where

I_{ysp} = the moment of inertia about the y axis through the suspension point

For a load with a rectangular shape, the moment of inertia can be approximated as

$$I_{ysp} = \frac{1}{6}mbh + ml^2$$

where

b= the base of the box

h= the height of the box

m= the mass of the load

Substituting I_{ysp} into the equation gives

$$\left(\frac{1}{6}mbh + ml^2\right)\ddot{\alpha} =$$

$$D_U l cos\alpha - D_W l sin\alpha - \big(mgcos(\theta)\big)(lsin\alpha) - \big(mgsin(\theta)\big)(lcos\alpha)$$

Substituting D_U and D_W and solving for $\ddot{\alpha}$ gives

$$\ddot{\alpha} = \frac{1}{\frac{1}{6}mbh+ml^2}\big[-mgl(sin\theta cos\alpha + cos\theta sin\alpha) + C_U l sign(U_L){U_L}^2 cos\alpha -$$

$$CWlsignWLWL2sin\alpha \qquad (3.7)$$

Forces in longitudinal and vertical directions gives

$$m\dot{U}_L = T_U - D_U + mgsin(\theta)$$

$$m\dot{W}_L = -T_W + D_W + mgcos(\theta)$$

Substituting D_U and D_W and solving for T_U and T_W gives

$$T_U = m\dot{U}_L + C_U sign(U_L){U_L}^2 - mgsin\theta \qquad (3.8)$$

$$T_W = -m\dot{W}_L + C_W sign(W_L){W_L}^2 + mgcos\theta \qquad (3.9)$$

3.4 Combined Model

To combine both models, the cable tension is added to the helicopter and its effect analysed, Figure 3.3. The load is considered to be hanging directly below the helicopter center of gravity so that in hover and without load motion, there are no moments created. This is the case for the Bell UH-1H helicopter that is used for simulation (Heffley, Jewell, Lehman, & Van Winkle, 1979)(Multiservice Helicopter Sling Load: Basic Operations and Equipment, 1997).

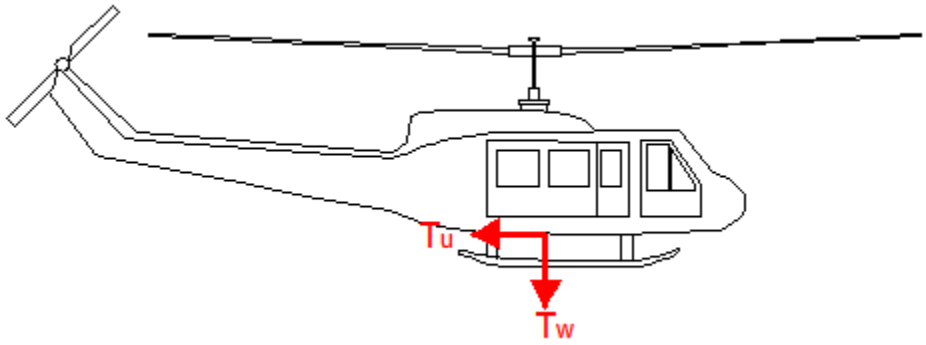

Figure 3-3 Helicopter with cable tension

The accelerations experienced by the helicopter without a load are given by the original model, and the effects of T_U and T_W are added the following way

$$\dot{U} = \dot{U}_H - \frac{1}{M} T_U \tag{3.10}$$

$$\dot{W} = \dot{W}_H + \frac{1}{M} T_W \tag{3.11}$$

$$\dot{Q} = \dot{Q}_H - \frac{z_{cg}}{I_y} T_U \tag{3.12}$$

where

M= the helicopter mass

$\dot{U}_H$= the helicopter longitudinal acceleration without a load (original model)

$\dot{W}_H$= the helicopter vertical acceleration without a load

$\dot{Q}_H$= the helicopter pitch angular acceleration without a load

I_y= the helicopter moment of inertia about the y axis

z_{cg}= the vertical distance from the center of gravity to the suspension point

Substituting T_U and T_W gives

$$\dot{U} = \dot{U}_H - \frac{1}{M}\left[m\dot{U}_L + C_U sign(U_L){U_L}^2 - mgsin\theta\right]$$

$$\dot{W} = \dot{W}_H + \frac{1}{M}\left[-m\dot{W}_L + C_W sign(W_L){W_L}^2 + mgcos\theta\right]$$

$$\dot{Q} = \dot{Q}_H - \frac{z_{cg}}{I_y}\left[m\dot{U}_L + C_U sign(U_L){U_L}^2 - mgsin\theta\right]$$

Substituting $\dot{U}_L$ and $\dot{W}_L$ and solving for $\dot{U}$, $\dot{W}$ and $\dot{Q}$

$$\dot{U} = \frac{M}{M+m}\dot{U}_H - \frac{1}{M+m}\left[ml(sin\alpha\dot{\alpha}^2 - cos\alpha\ddot{\alpha}) + C_U sign(U_L){U_L}^2 - mgsin\theta\right] \tag{3.13}$$

$$\dot{W} = \frac{M}{M+m}\dot{W}_H + \frac{1}{M+m}\left[ml(cos\alpha\dot{\alpha}^2 + sin\alpha\ddot{\alpha}) + C_W sign(W_L){W_L}^2 + \right. \tag{3.14}$$

$$mgcos\theta]$$

$$\dot{Q} = \dot{Q}_H - \frac{z_{cg}}{I_y}\left[m\left(\dot{U} - l(cos\alpha\ddot{\alpha} - sin\alpha\dot{\alpha}^2)\right) + C_U sign(U_L){U_L}^2 - \right. \quad (3.15)$$

$$mgsin\theta$$

The system is augmented to a 10th order system, with the addition of the load angle (α) and load angle rate ($\dot{\alpha}$). It uses equations (3.7), (3.13), (3.14) and (3.15), while the other states remain unchanged from the original helicopter model.

3.5 Linearization

The new model defined in section 3.4 represents a non-linear system and must be linearized in order to apply linear control theory. To accomplish this, the procedure described in (Williams & Lawrence, 2007) was employed.

For a non linear system

$$\dot{x}(t) = f[x(t), u(t), t] \quad (3.16)$$

$$y(t) = h[x(t), u(t), t] \quad (3.17)$$

where $\dot{x}(t)$ and $y(t)$ are continuously differentiable functions. Linearization is performed about a nominal trajectory or operating point; where for a nominal input signal, $\tilde{u}(t)$, the nominal state trajectory and the nominal output trajectory satisfy

$$\dot{\tilde{x}}(t) = f[\tilde{x}(t), \tilde{u}(t), t] \tag{3.18}$$

$$\dot{\tilde{y}}(t) = h[\tilde{x}(t), \tilde{u}(t), t] \tag{3.19}$$

Deviations of the state, input and output from their nominal trajectories are denoted by the δ subscripts via

$$x_\delta(t) = x(t) - \tilde{x}(t) \tag{3.20}$$

$$u_\delta(t) = x(t) - \tilde{x}(t) \tag{3.21}$$

$$y_\delta(t) = y(t) - \tilde{y}(t) \tag{3.22}$$

If $\tilde{u}(t) = \tilde{u}$, a constant vector, there exists a special case of equilibrium state $\tilde{x}$ that for all t satisfies

$$0 = f[\tilde{x}, \tilde{u}, t] \tag{3.23}$$

and the input and output remain close to their respective nominal trajectories, the system can be

expressed in the linearized form

$$\dot{x}_\delta(t) = A(t)x_\delta(t) + B(t)u_\delta(t) \tag{3.24}$$

$$y_\delta(t) = C(t)x_\delta(t) + D(t)u_\delta(t) \tag{3.25}$$

where the coefficient matrices are defined as

$$A(t) = \frac{df}{dx}[\tilde{x}(t), \tilde{u}(t), t] \tag{3.26}$$

$$B(t) = \frac{df}{du}[\tilde{x}(t), \tilde{u}(t), t] \tag{3.27}$$

$$C(t) = \frac{dh}{dx}[\tilde{x}(t), \tilde{u}(t), t] \tag{3.28}$$

$$D(t) = \frac{dh}{du}[\tilde{x}(t), \tilde{u}(t), t] \tag{3.29}$$

The linearized equations used in this thesis are shown in Appendix A

3.6 Operating Point Selection

The operating points for the simulation of a Bell 205 (UH-1H) helicopter, were chosen to match those presented in (Heffley, Jewell, Lehman, & Van Winkle, 1979). The linear velocities are selected the same as those presented in the document. To meet the criteria defined in Equation (3.23) the system equations are equaled to zero and the nominal state and input values are calculated. The nominal helicopter angular rates as well as the nominal load angle rate are set as zero. The values for the remaining nominal point states and nominal control inputs were determined by numerical calculations and are specific to each mass and cable length combination. The three operating points selected were hover for which the nominal state values are

$$\tilde{U} = 0.51, \tilde{V} = 0.00, \tilde{W} = 0.04$$

$$\tilde{P} = 0.00, \tilde{Q} = 0.00, \tilde{R} = 0, \tilde{\alpha} = 0.00$$

10 knots forward velocity for which the nominal state values are

$$\widetilde{U} = 5.13, \tilde{V} = -0.01, \widetilde{W} = 0.35$$

$$\tilde{P} = 0.00, \tilde{Q} = 0.00, \tilde{R} = 0.00, \tilde{\alpha} = 0.00$$

and 20 knots forward velocity for which the nominal state values are

$$\widetilde{U} = 10.27, \tilde{V} = -0.01, \widetilde{W} = 0.66$$

$$\tilde{P} = 0.00, \tilde{Q} = 0.00, \tilde{R} = 0.00, \tilde{\alpha} = 0.00$$

The expanded model for the Bell 205 helicopter in hover, with a 500 kg load suspended from a 6 m cable, is described by

$$A_{hover} = \begin{bmatrix} 0 & 0.02 & 0.16 & -0.01 & -0.37 & -0.07 & -6.24 & 0 & -1.19 & 0 \\ -0.09 & -0.34 & 0.08 & -0.09 & -0.11 & 0.59 & -0.02 & 0 & 0.03 & 0 \\ 0.01 & -0.01 & -0.20 & 0 & 0.26 & 0.04 & 0.39 & 0 & -0.54 & 0 \\ 0.02 & 0 & -0.41 & -0.05 & -0.27 & 0.27 & 0 & 9.81 & 0 & 0 \\ 0.03 & -0.02 & -0.88 & -0.04 & -0.57 & 0.14 & 0 & 0 & 0 & 0 \\ -0.01 & -0.02 & -0.06 & 0.07 & -0.32 & -0.71 & 0 & 0 & 0 & 0 \\ 0 & 0 & 1 & 0 & 0 & 0 & 0 & 0 & 0 & 0 \\ 0 & 0 & 0 & 0 & 1 & 0 & 0 & 0 & 0 & 0 \\ 0 & 0 & 0 & 0 & 0 & 0 & 0 & 0 & 0 & 1 \\ 0 & 0 & 0 & 0 & 0 & 0 & 1.63 & 0 & -1.63 & 0 \end{bmatrix}$$

$$B_{hover} = \begin{bmatrix} 0.07 & 0.11 & 0 & 0 \\ -1.03 & 0.03 & 0 & 0.01 \\ 0 & -0.07 & 0 & 0.01 \\ -0.04 & 0 & 0.11 & 0.20 \\ -0.04 & 0 & 0.22 & 0.17 \\ 0.17 & 0 & 0.03 & -0.47 \\ 0 & 0 & 0 & 0 \\ 0 & 0 & 0 & 0 \\ 0 & 0 & 0 & 0 \\ 0 & 0 & 0 & 0 \end{bmatrix}$$

The expanded model for the Bell 205 helicopter in 10 knots forward flight, with a 500 kg load suspended from a 6 m cable, is described by

$$A_{10k}$$

$$= \begin{bmatrix} 0 & 0.03 & 0.22 & 0 & -0.37 & -0.07 & -6.25 & 0 & -1.19 & 0 \\ -0.16 & -0.39 & 0.30 & -0.05 & -0.16 & 0.55 & -0.01 & 0 & 0.02 & 0 \\ 0.01 & -0.01 & -0.28 & 0.01 & 0.26 & 0.03 & 0.39 & 0 & -0.54 & 0 \\ 0.01 & 0 & -0.42 & -0.05 & -0.33 & 0.27 & 0 & 9.81 & 0 & 0 \\ 0.02 & -0.01 & -0.86 & -0.04 & -0.69 & 0.14 & 0 & 0 & 0 & 0 \\ -0.02 & -0.02 & -0.03 & 0.07 & -0.31 & -0.73 & 0 & 0 & 0 & 0 \\ 0 & 0 & 1 & 0 & 0 & 0 & 0 & 0 & 0 & 0 \\ 0 & 0 & 0 & 0 & 1 & 0 & 0 & 0 & 0 & 0 \\ 0 & 0 & 0 & 0 & 0 & 0 & 0 & 0 & 0 & 1 \\ 0 & 0 & 0 & 0 & 0 & 0 & 1.63 & 0 & -1.63 & 0.01 \end{bmatrix}$$

$$B_{10k} = \begin{bmatrix} 0.07 & 0.11 & 0 & 0 \\ -1.00 & 0.05 & 0 & 0 \\ -0.01 & -0.07 & 0 & 0 \\ -0.03 & 0 & 0.11 & 0.19 \\ -0.03 & 0.01 & 0.22 & 0.16 \\ 0.16 & 0 & 0.03 & -0.46 \\ 0 & 0 & 0 & 0 \\ 0 & 0 & 0 & 0 \\ 0 & 0 & 0 & 0 \\ 0 & 0 & 0 & 0 \end{bmatrix}$$

The expanded model for the Bell 205 helicopter in 20 knots forward flight, with a 500 kg load suspended from a 6 m cable, is described by

$$A_{20k} = \begin{bmatrix} 0 & 0.03 & 0.29 & 0 & -0.35 & -0.06 & -6.25 & 0 & -1.19 & 0 \\ -0.17 & -0.50 & 0.31 & -0.03 & -0.19 & 0.50 & 0.03 & 0 & -0.03 & 0 \\ 0 & -0.01 & -0.31 & 0.01 & 0.25 & 0.02 & 0.39 & 0 & -0.54 & 0 \\ 0.01 & 0 & -0.41 & -0.07 & -0.41 & 0.27 & 0 & 9.81 & 0 & 0 \\ 0.01 & -0.01 & -0.82 & -0.04 & -0.82 & 0.14 & 0 & 0 & 0 & 0 \\ -0.03 & -0.02 & 0.11 & 0.07 & -0.28 & -0.74 & 0 & 0 & 0 & 0 \\ 0 & 0 & 1 & 0 & 0 & 0 & 0 & 0 & 0 & 0 \\ 0 & 0 & 0 & 0 & 1 & 0 & 0 & 0 & 0 & 0 \\ 0 & 0 & 0 & 0 & 0 & 0 & 0 & 0 & 0 & 1 \\ 0 & 0 & 0 & 0 & 0 & 0 & 1.63 & 0 & -1.63 & -0.03 \end{bmatrix}$$

$$B_{20k} = \begin{bmatrix} 0.06 & 0.11 & 0 & 0 \\ -0.98 & 0.09 & 0 & 0 \\ -0.01 & -0.07 & 0 & 0 \\ -0.02 & 0 & 0.11 & 0.17 \\ -0.01 & 0.01 & 0.22 & 0.14 \\ 0.14 & -0.01 & 0.03 & -0.41 \\ 0 & 0 & 0 & 0 \\ 0 & 0 & 0 & 0 \\ 0 & 0 & 0 & 0 \\ 0 & 0 & 0 & 0 \end{bmatrix}$$

Chapter 4 Controller Synthesis

4.1 Introduction

The design process consists of a model following controller synthesis that attempts to copy an ideal model derived from the ADS-33 specified level 1 handling qualities. It is desired to use a Linear Quadratic Regulator (LQR), because it reduces the control power usage and guarantees stability; however, it does not achieve the desired behaviour. Thus, it is necessary to modify the LQR design process so that it controls the error between the helicopter response and an ideal model, driving it to zero. There are two different design techniques (Stevens & Lewis, 1992): explicit model following (EMF), in which the target model appears in the controller and implicit model following (IMF), in which only a description of the model is used in the design process. Trentini (Trentini, 1999) states that the EMF with command generator tracker technique (CGT) is the option best suited for this application as it provides good performance with acceptable control effort.

4.2 Linear Quadratic Regulator Theory

Among the most commonly employed control techniques are the state feedback design, in which the states are fed back to the controller where appropriate action is calculated and applied. The linear Quadratic Regulator (LQR) is a special type of feedback controller where the states are multiplied by a constant and used as the system

input without the use of a reference signal, Figure 4-1. The main advantage of using an LQR is that it is an optimum controller, meaning it provides corrective action with minimum control power usage. It can be applied to a fully controllable state space system of the form

$$\dot{x} = Ax + Bu \tag{4.1}$$

by applying the control signal

$$u = -Kx \tag{4.2}$$

By doing this, the closed loop system becomes

$$\dot{x} = Ax + B(-Kx)$$

$$\dot{x} = (A - BK)x$$

$$\dot{x} = A_C x \tag{4.3}$$

where

A_C = the closed loop system matrix

It is important to notice that the new system does not explicitly follow a reference signal, but instead tries to reduce the states driving them to zero. This type of controller is referred to as regulator, as opposed to a tracker, which follows a reference signal that is usually non-zero.

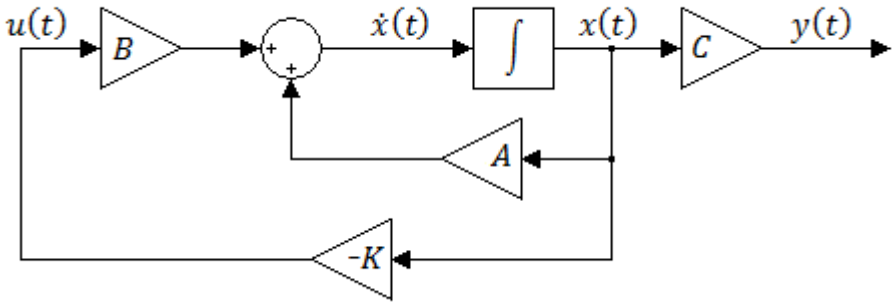

Figure 4-1 LQR controller

To solve for the optimum controller, the LQR problem consists in finding the optimum gain matrix K that minimizes the system performance index. For instances when it is desired that the states go to zero at time T with initial time τ, the performance index is described by

$$J = \int_{\tau}^{T} x^T Q x + u^T R u \, dt \tag{4.4}$$

Often it is desired to find a steady state solution where T goes to infinity instead of a set time. For those cases, the performance index can be expressed as

$$J = \frac{1}{2}\int_{0}^{\infty} x^T Q x + u^T R u \, dt \tag{4.5}$$

After substituting the control signal u, the performance index becomes

$$\frac{1}{2}\int_{0}^{\infty} x^T (Q + K^T R K) x \, dt \tag{4.6}$$

To find the optimal feedback matrix K for a steady state case, suppose there is a constant value P such that

$$\frac{d}{dt}(x^T P x) = -x^T (Q + K^T R K) x \tag{4.7}$$

And substituting into the performance index gives

$$J = -\frac{1}{2}\int_0^\infty \frac{d}{dt}(x^T P x)\, dt$$

$$J = \frac{1}{2}x^T(0) P x(0)$$

where it is assumed that the system is stable and, thus, x(t) goes to zero as t goes to infinity. Doing this means that the performance index is now independent of the gain matrix K and only depends on the constant P. Next, it is necessary to find a gain matrix K so that (4.7) holds true. To do this, first differentiate (4.7), which gives

$$\dot{x}^T P x + x^T P \dot{x} + x^T Q x + x^T K^T R K x = 0$$

$$x^T {A_C}^T P x + x^T P A_C x + x^T Q x + x^T K^T R K x = 0$$

$$x^T \left({A_C}^T P + P A_C + Q + K^T R K\right) x = 0$$

In order for this to hold true, the term inside the parenthesis must equal zero

$${A_C}^T P + P A_C + Q + K^T R K = 0$$

Substituting Ac

$$(A - BK)^T P + P(A - BK) + Q + K^T RK = 0$$

$$A^T P + PA + Q + K^T RK - K^T B^T P - PBK = 0$$

Selecting K as

$$K = R^{-1} B^T P \tag{4.8}$$

Yields

$$A^T P + PA + Q + PBR^{-1} B^T P = 0 \tag{4.9}$$

The result is an Algebraic Riccati Equation (ARE) which can be solved for P, given A, B, Q and R. The task then becomes selecting the appropriate Q and R matrices that provide the desired performance. Notice that the performance index takes into account both the control signals as well as the system states. The weighting matrix Q is used to define the behaviour of the states, as a large Q requires a small x in order to keep the performance index small. Likewise, R is used for the control signal, as a large R requires a small u in order to keep the performance index small. This means that larger values of Q generally result in the poles of the closed-loop system matrix *AC* being further left in the s-plane so that the state decays faster to zero. On the other hand, a

larger R means that less control effort is used, so that the poles are generally slower, resulting in larger values of the state x.

Certain restrictions must be met for the LQR design to be applicable. The open loop system described by A and B must be fully controllable. There are also restrictions for the selection of the weighting matrices. Q is to be selected as positive semi-definite and R as positive definite. This means that the value of $x^T Qx$ should always be positive or zero and $u^T Ru$ should always be positive to ensure that the performance index is well defined. R has to always be positive definite because it has to be invertible.

Summary of LQR design procedure

1. Check controllability of A and B
2. Select appropriate Q and R matrices
3. Solve the ARE for P
4. Calculate the optimum gain matrix K

4.3 LQR Evaluation

The linear Quadratic Regulator provides many desired properties for the controller; however, it does not satisfy all of them. One of the good qualities that it offers is: it provides a solution with minimum control power usage, which leads to a reduction in helicopter power requirements and a reduction in fuel consumption. This is a desired

property when dealing with the aerospace industry where operation costs can be in the thousands of dollars per hour (Conklin & de Decker Associates, Inc, 2012) with a major component being of fuel (Conklin & de Decker Associates, Inc, 2012), as aircrafts require special fuel which is generally of a higher grade than in less critical applications (Air BP, 2012). Another advantage of low control energy usage is that it maintains the control signals and actuators action low. There is a finite amount of actuation that can be applied and if the control signals are too large, then the actuators will not be able to provide the desired response and the system will not stabilize. Because of this it is important to keep the energy usage and control signals low and realistic.

One the properties of the LQR that does not meet the desired behaviour, is that it does not explicitly follow a reference signal; instead it drives the states to zero. This means that the controller does not provide the desired response. If the helicopter was to remain hovering at all times, this would be a good solution as it would try to get everything to stop moving and remain in one spot. For this project, the inability to follow a reference signal is a problem as the helicopter must respond accordingly with the pilot inputs when in forward flight.

The LQR controller also does not provide the desired behaviour described by the ADS-33 handling qualities specifications. One of the problems is that it does not explicitly decouple the different axes. For example, if the pilot wants to go straight up, the controller has to provide collective action. As was mentioned in Section 2.3, when anti-torque action is applied, it results in a variation of power output by the main rotor

and, unless collective action is also applied, the helicopter will move vertically. Because the steady state LQR provides a solution for the final value of the states be zero, not the intermediate values, it will allow the helicopter to move vertically while rotating about its yaw axis until reaching the desired attitude. Because of these issues it is necessary to find a solution that will provide the desired helicopter behaviour.

4.4 Model Following Controller

It is desired to use a Linear Quadratic Regulator (LQR); however, it does not provide the desired behaviour. Thus, it is necessary to find another solution in order to achieve the desired results. One way to accomplish this is to modify the LQR design process so that it controls the error between the helicopter response and the ideal model, driving it to zero. This takes advantage of the LQR property that drives the states to zero, a former setback, and turns it into a solution to the problem.

There are two different model following design techniques (Stevens & Lewis, 1992): explicit model following (EMF), in which the target model appears in the controller and implicit model following (IMF), in which only a description of the model is used in the design process. Trentini(Trentini, 1999) states that the EMF with command generator tracker (CGT) technique is the option best suited for helicopter controller design as it provides good performance with acceptable control effort.

4.4.1 Ideal target model

The ideal target model is derived from the ADS-33 specified handling qualities for level 1 flight. The specifications depend on the task that is required to perform, Mission Task Elements (MTE), and the environment in which it must be done, Usable Cue Environment (UCE). The UCE range from 1 to 3, where 1 is normal daylight visual environment and 3 is extremely poor visual environment. For acceleration and deceleration (depart/abort) in a UCE 2, ADS-33 calls for attitude command attitude hold (ACAH) response in pitch and roll axes and rate command heading hold (RCHH) in vertical and yaw axes.

As mentioned in Sections 2.5.3 and 2.5.4, for level 1 handling qualities, the small amplitude response for pitch and roll axes should be ACAH with a bandwidth of at least 3 rad/s. The cross-coupling between these axes is limited by the maximum ratio of off-axis response to on-axis command, which must be less than 0.25. For the yaw axis, the small amplitude response should be RCHH with a bandwidth of at least 3 rad/s. Cross-coupling for yaw axis and collective control must be less than 15%. The time constant of the first order vertical rate response shall not be less than 0.2 s^{-1}. Cross-coupling between the vertical and yaw axes should be less than 10%.

Based on the requirements mentioned above, a low order closed loop system with zero cross-coupling behaviour is selected for the target model. Forward, lateral, vertical and yaw rates are specified as first order equations

$$\dot{U} = -\lambda_U U - \lambda_U \theta$$

$$\dot{V} = -\lambda_V V + \lambda_V \phi$$

$$\dot{W} = -\lambda_W W + \lambda_W r_W$$

$$\dot{R} = -\lambda_R R + \lambda_R r_R$$

The pitch and roll attitude responses must take into account the pitch and roll rates, thus giving second order response characteristics

$$\dot{Q} = -2\zeta_\theta \omega_\theta Q - \omega_\theta^2 \theta - \omega_\theta^2 r_\theta$$

$$\dot{P} = -2\zeta_\phi \omega_\phi P - \omega_\phi^2 \phi - \omega_\phi^2 r_\phi$$

Combining these equations into a state space model yields the ideal target model

$$\underline{\dot{x}} = \underline{Ax} + \underline{B}r \tag{4.10}$$

The ideal model is guided by the reference input *r*, which applies to the vertical velocity, pitch attitude, roll attitude and yaw rate. The target model contains the same states as the expanded helicopter model and uses the equations defined above with the following values

$$\lambda_U = 4.0,\ \lambda_V = 4.0,\ \lambda_W = 3.0,\ \lambda_R = 5.0$$

$$\zeta_\theta = 0.7,\ \zeta_\phi = 0.7,\ \omega_\theta = 4.0,\ \omega_\phi = 4.0$$

which are defined to meet, and often exceed, the requirements described in Sections 2.5.3 and 2.5.4.

For the suspended load, as will be shown in Section 4.4.2, its response cannot be modified to follow and ideal behaviour and no handling qualities are specified for it in the ADS- 33. For these reasons, an ideal behaviour was not developed for it.

4.4.2 EMF with CGT Design

The design process begins by selecting the performance outputs to be used when defining the mismatch error the controller attempts to reduce. Since the helicopter has four control inputs, only four states can be independently controlled and, as mentioned in Section 4.4.1, these states should be vertical rate, pitch attitude, roll attitude and yaw rate. This means that with this method the load cannot be controlled to follow an ideal response; however, as will be shown in Section 4.5, its behaviour can still be modified. The selected performance outputs are

$$z = Hx = \begin{bmatrix} W \\ \theta \\ \phi \\ R \end{bmatrix} = \begin{bmatrix} vertical\ velocity \\ pitch\ attitude \\ roll\ attitude \\ yaw\ rate \end{bmatrix}$$

where

$$H = \begin{bmatrix} 0 & 1 & 0 & 0 & 0 & 0 & 0 & 0 & 0 & 0 \\ 0 & 0 & 0 & 0 & 0 & 0 & 1 & 0 & 0 & 0 \\ 0 & 0 & 0 & 0 & 0 & 0 & 0 & 1 & 0 & 0 \\ 0 & 0 & 0 & 0 & 0 & 1 & 0 & 0 & 0 & 0 \end{bmatrix}$$

To produce the forced response, the target model performance outputs are chosen the same as those for the plant

$$\underline{z} = \underline{Hx} = H\underline{x}$$

The mismatch error is defined as

$$e = \underline{z} - z = \underline{Hx} - Hx \tag{4.11}$$

The plant and ideal model are combined into the following augmented system

$$\dot{x'} = A'x' + B'u + G'r \tag{4.12}$$

where

$$A' = \begin{bmatrix} A & 0 \\ 0 & \underline{A} \end{bmatrix},\ B' = \begin{bmatrix} B \\ 0 \end{bmatrix}$$

$$G' = \begin{bmatrix} 0 \\ \underline{B} \end{bmatrix},\ x' = \begin{bmatrix} x \\ \underline{x} \end{bmatrix}$$

It is clear that this is a tracking problem and regulator theory cannot be applied. Thus, it must be modified using the CGT technique, where the reference signal *r(t)* satisfies the differential equation

$$r^d + a_1 r^{d-1} + \cdots + a_d r = 0 \tag{4.13}$$

for an appropriate differential order d and coefficient set a_i. A useful case is when d and a_i are set to 1 and 0, respectively, yielding the unit step

$$\dot{r} = 0,\ r(0) = r_0 \tag{4.14}$$

The command generator characteristic polynomial is defined as

$$f(s) = s^d + a_1 s^{d-1} + \cdots + a_d s$$

or in the case described in (4.14)

$$f(s) = s \tag{4.15}$$

Performing this operation on the augmented system (4.12) produces the modified system

$$\dot{\varepsilon} = A'\varepsilon + B'\mu \tag{4.16}$$

where

$$\varepsilon = f(x') = \dot{x}'$$

$$\mu = f(u) = \dot{u}$$

and more importantly

$$f(r) = \dot{r} = 0$$

Applying the operation (4.15) to the mismatch error gives

$$f(e) = \dot{e}$$

$$f(e) = H'\varepsilon$$

where

$$H' = [-H \quad \underline{H}]$$

Representing the error in state variable form

$$\dot{e} = Fe + H'\varepsilon \tag{4.17}$$

where *F=0*, with the appropriate dimensions.

Finally, collecting the augmented helicopter system and mismatch error into a single system produces

$$\dot{\varepsilon'} = \tilde{A}\varepsilon' + \tilde{B}\mu$$

$$\begin{bmatrix} \dot{e} \\ \dot{\varepsilon} \end{bmatrix} = \begin{bmatrix} F & H' \\ 0 & A' \end{bmatrix} \begin{bmatrix} e \\ \varepsilon \end{bmatrix} + \begin{bmatrix} 0 \\ B' \end{bmatrix} \mu \tag{4.18}$$

The final system produced is no longer driven by the reference signal and so regulator theory can be applied. The design process becomes finding appropriate Q and R weighting matrices to produce the desired controller that drives the states, including the

mismatch error, to zero. The resulting gain matrix K can be divided into K_1 and K_2 and applied to the mismatch error and plant and ideal model separately

$$K\varepsilon' = K_1 e + K_2 \varepsilon$$

It is important to remember that the pseudo-controller (μ) cannot be applied to the system which it is driven by u. To find the true control input, integration of μ is necessary

$$u = \int \mu \, dt = \int K_1 e + K_2 \varepsilon \, dt$$

$$u = H' K_1 \int x' \, dt + K_2 x' \tag{4.19}$$

4.5 Load stability control

While the controller described above ensures helicopter performance, it appears to ignore the under-slung load. This is not the case. Proper design can create a controller that can also reduce the load oscillations. Typically, when designing a model following controller, high control effort is applied to the mismatch error and little, if any, to the other states. The target model states are driven by the reference signal, so nothing is gained by applying control effort as it does not modify them. For the plant model, the design goal is to have the mismatch error drive it. Applying control effort to the states can create conflicting commands, where the regulator drives them to zero while the mismatch error drives them to another value.

For this particular application, it is possible to apply strong control effort to the load angle rate and not create conflicting commands. As was mentioned in section 4.4.2, the mismatch error does not consider the suspended load and does not drive it to a desired behavior. Because of the drag forces, the load goes to a set angle and while that value cannot be modified the motion can be dampened so its final position is reached with less oscillation. Thus, applying control effort to the load angle rate acts as a Load Stability Control (LSC).

A regular model following controller was designed without the LSC. The weighting matrices Q and R are chosen first to approximate an existing model following controller for a helicopter without a suspended load. They are chosen based on an inverse squared rule (Astrom & Wittenmark, 1990), where the matrices are selected as diagonal with element values that normalize contributions based on maximum deviation in the corresponding state or input. Once a satisfactory controller has been found, the LSC value for the load angle rate is found. The process is done in this order because the most important thing is to ensure that the helicopter behaviour meets the ADS-33 guidelines.

One of the setbacks of using strong control effort to reduce the load swinging is that the helicopter behaviour must be adjusted, altering the plant response and deviating it from the ideal model. It is important to verify that the LSC does not severely affect the helicopter model following performance and that it remains close to the ideal model.

Chapter 5 Simulation Results

5.1 Simulation Setup

To test the controller, simulations were conducted for a Bell 205 (UH-1H) helicopter with an attached load using the model derived in Chapter 3, with the simulation software Matlab and Simulink. The simulations consisted in the acceleration of the helicopter from hover to a forward velocity of 10 m/s, holding that velocity for a 30 s and then returning to hover. The acceleration and stopping are achieved through pitch attitude commands. The helicopter is pitched -0.5 rad while accelerating and takes 22.5s to reach the desired velocity.

The trimmed operating conditions used were hover, 10 knots (5.1 m/s) forward flight and 20 knots (10.2 m/s) forward flight, with a mid-range weight (3629 kg). The models are taken from (Heffley, Jewell, Lehman, & Van Winkle, 1979) and are expanded using the equations derived in Chapter 3. Switching between the hover and 10 knots models occurred when the forward velocity reached 2.5 m/s. Switching between the 10 knots and 20 knots models occurred when the forward velocity reached 7.5 m/s. The system uses one controller derived from the 10 knots model as this is the middle condition and provides good control for the other trim conditions.

To approximate the drag forces experimented by the load, the simulation considers the air density to be 1.112 kg/m3, which is the density in Calgary (1000 m

altitude) at 0°C. The load is simulated as a one meter cubed box with the air striking the face of the box, not the edge. Based on this and the information provided in Table 1, the drag coefficient is approximated to 1.1.

A maximum load of 500 kg was selected to ensure that the helicopter maximum payload (4309 kg) is not exceeded. Cargo loads are recommended to be at least 227 kg, as low masses tend to deploy toward the horizontal, with the risk of striking the tail rotors (Helicopter External Load Operations, 2006). For this reason masses for simulation are selected as 250 kg and 500 kg. Sling load cables are usually 6 m long; however, roundslings of up to 20 m can be attached to increase the clearance between the helicopter and the (Multiservice Helicopter Sling Load: Basic Operations and Equipment, 1997). For this reason, the cable lengths were selected from 6 m to 26 m as this provides a realistic range of lengths.

Adequate saturation limits were set for the control inputs based on the cockpit command levers full range of travel. Heffley (Heffley, Jewell, Lehman, & Van Winkle, 1979) specified that the full range of travel for the command levers is 27.2 cm for main rotor collective, 33.0 cm for both longitudinal and lateral cyclic and 16.5 cm for the tail rotor pedals. Because of this, the saturation limits were set as ±13.6 cm for main rotor collective, ±16.5 cm for both longitudinal and lateral cyclic and ±8.2 cm for the tail rotor pedals. It is assumed that the middle position corresponds with the null command and is thus set as zero. This saturation ensures that the deflection limits of the actuators are not exceeded, regardless of the signals generated by the controller.

A regular model following controller was designed without the LSC. The weighting matrices Q and R are chosen first to approximate an existing model following controller for a helicopter without a suspended load. They are chosen based on an inverse squared rule (Astrom & Wittenmark, 1990), where the matrices are selected as diagonal with element values that normalize contributions based on maximum deviation in the corresponding state or input.

For R, the values depend on the maximum expected deviations of the control signal u. Based on the saturation limits defined above, the maximum expected control signal deviations are 13.6 cm for main rotor collective, 16.5 cm for both longitudinal and lateral cyclic and 8.2 cm for the tail rotor pedals. The weighting matrix R is then selected as:

$$R = diag\left(\frac{1}{13.6^2}, \frac{1}{16.5^2}, \frac{1}{16.5^2}, \frac{1}{8.2^2}\right)$$

For Q, the values depend on the maximum expected deviations of the state x. For this matrix, weight is only applied to the mismatch error states used for the model following control (the first four states); selecting a value of zero for all other states. They are selected this way to prevent conflicting commands, where the regulator drives the states to zero while the mismatch error drives them to another value. It is desired that the plant response remain within 0.1 m/s of the ideal response for the vertical rate, 0.01 rad for the pitch and roll attitudes and 0.01 rad/s for the yaw rate. Once a satisfactory controller has been found, the LSC value for the load angle rate is selected. The process

is done in this order because the most important thing is to ensure that the helicopter behaviour meets the ADS-33 guidelines. The LSC term is set to be 5% of the values used for the mismatch error, to ensure helicopter behaviour. The weight for the vertical rate is then set as 10000 to match that of the other three states, and the LSC is selected as 500. With this, the new Q matrix is the diagonal matrix

$$Q = diag\left(\frac{1}{0.01^2}, \frac{1}{0.01^2}, \frac{1}{0.01^2}, \frac{1}{0.01^2}, Q1\right)$$

$$Q = diag(10000, 10000, 10000, 10000, Q1)$$

where Q1 has a value of 500 for the load angle rate and zero for all others, with the appropriate dimensions.

5.2 Simulation Results

Simulations were realized for different load masses and cable lengths to check how these parameters affect the behaviour of the under-slung system. Loads of 500 kg and 250 kg are used along with cable lengths from 6 m to 26 m. The maximum load angle deflection when the helicopter returns to hover, without applying the LSC, is measured and plotted in Figure 5-1 for the different configurations. This instance was chosen because the oscillation is larger when the system stops than when it accelerates, as can be seen in Figure 5-2 through Figure 5-4.

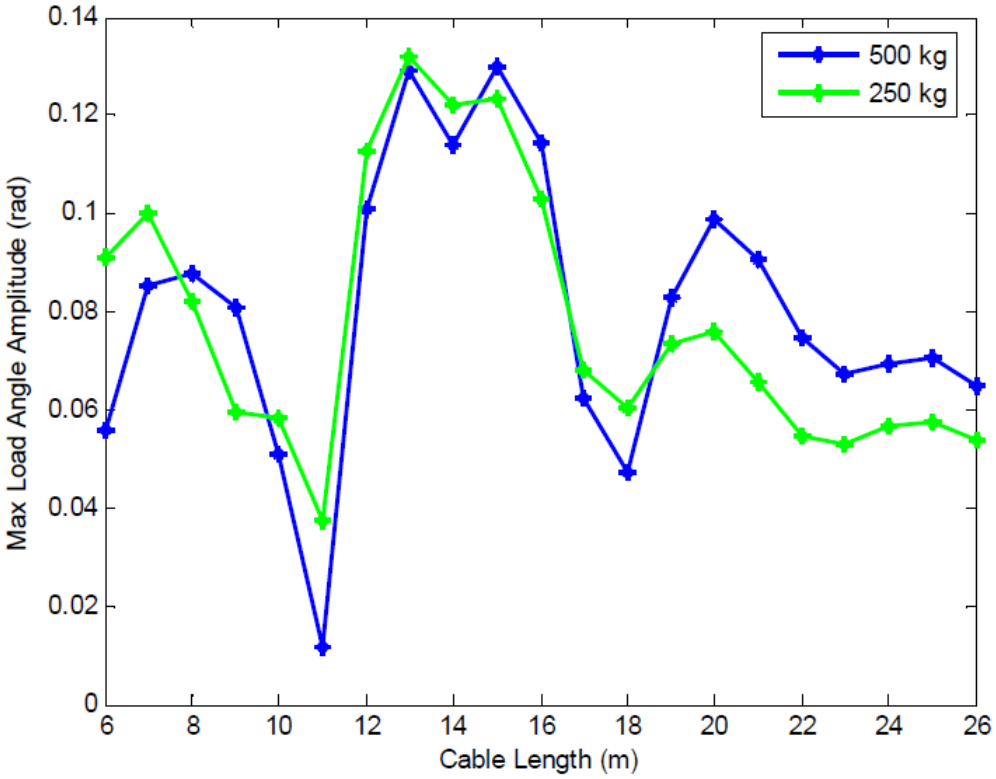

Figure 5-1 Max load angle deflection for different mass and cable length when stopping

Figure 5-1 shows that there is a fluctuating behaviour for the maximum load angle deflection with the largest variation taking place when the cable is between 10 m and 19 m. The largest peak is reached when the cable length is 13 to 15 m, and it's surrounded by two large drops at around 11 m and 18 m. Outside of the 10 m and 19m band, the behaviour is fairly consistent, with variations of less than 0.02 rad. When longer cables are used, the swing amplitude shows a decreasing tendency.

The 10 m to 19 m zone should be avoided as the system presents fluctuating behaviour and large variations of load oscillation. Despite this, the proposed controller

can still be used with any of the cables and will provide improvement in damping load oscillations.

Based on Figure 5-1, the cable lengths of 6 m, 13 m and 26 m are chosen to evaluate the behaviour of the system during the full simulation time, with the LSC. The load angle deflections for various masses and the three cable lengths are plotted in Figure 5-2 through Figure 5-4. The figures show that the suspended load swings at a higher frequency with shorter cables, while mass appears to have little effect on the frequency of oscillation. Also, a lower mass results in larger deflection than a higher mass.

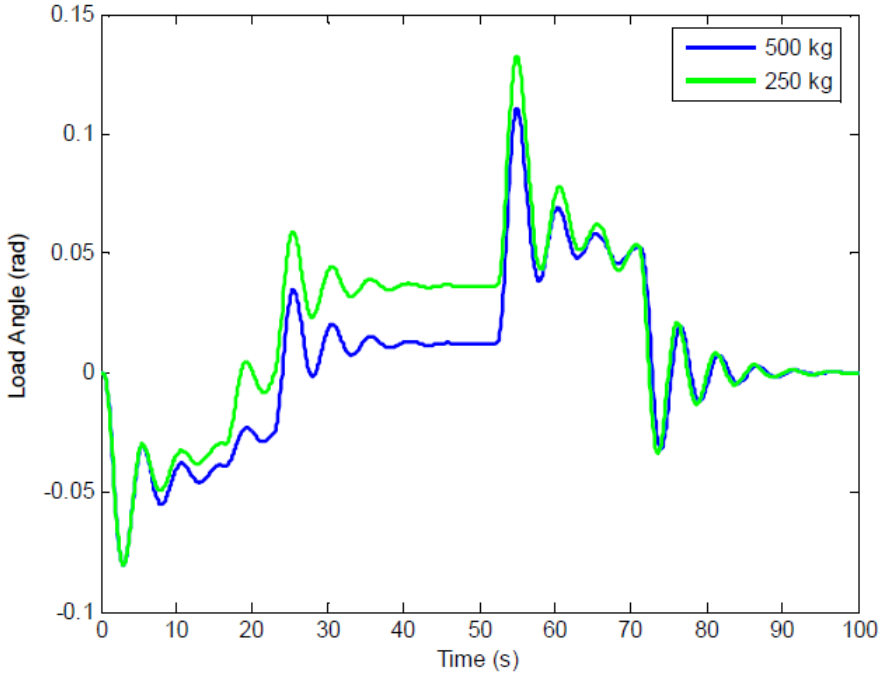

Figure 5-2 Load angle deflection for cable length of 6m

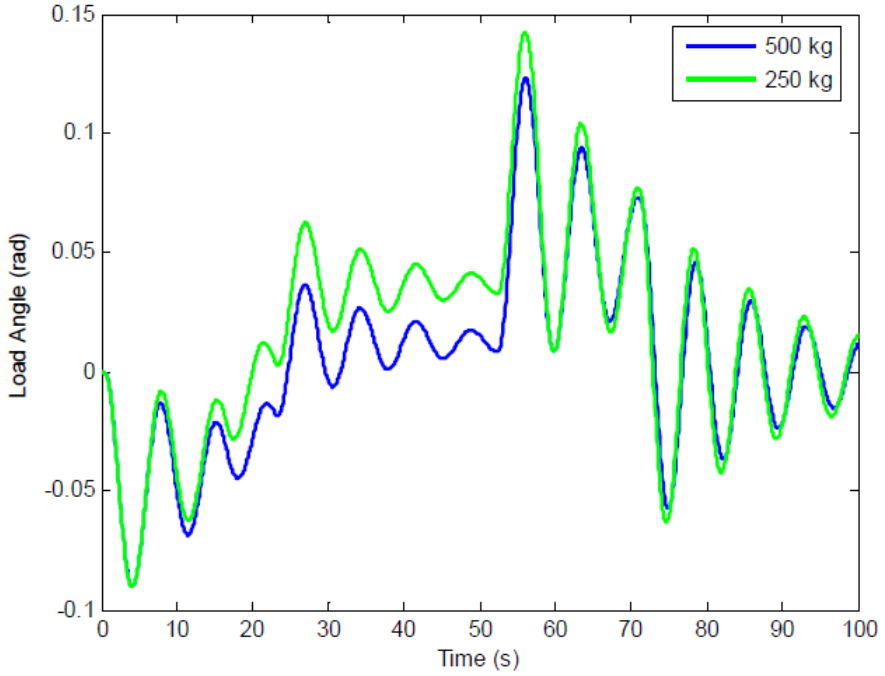

Figure 5-3 Load angle deflection for cable length of 13m

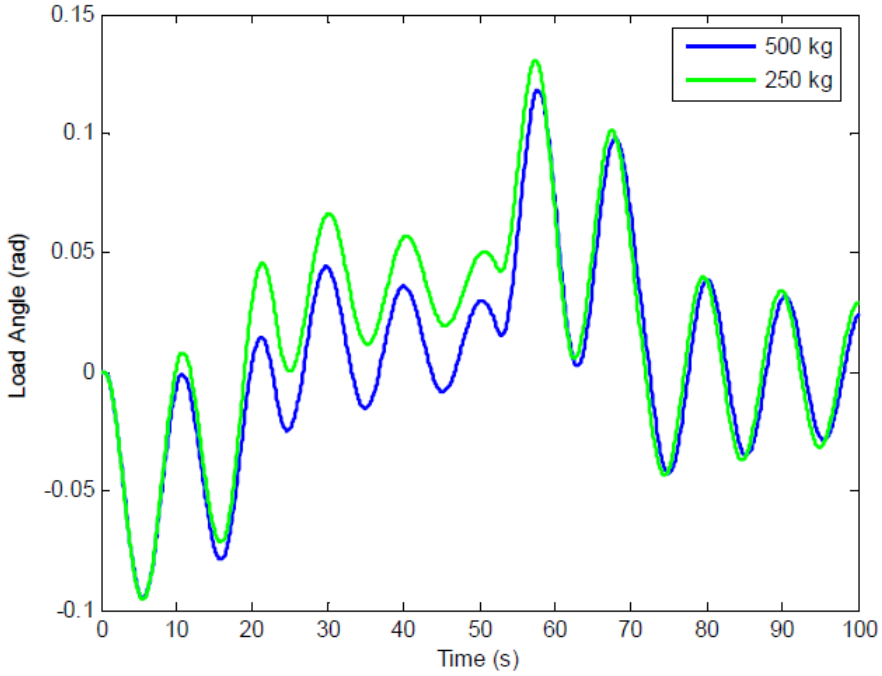

Figure 5-4 Load angle deflection for cable length of 26m

The same three cable lengths along with a mass of 500 kg are chosen to show the effect the LSC term has on the system behaviour. Simulations were conducted using the model following design with and without the LSC, for said configurations. As can be seen in Figure 5-5 through Figure 5-7, the implementation of the LSC term to the model following design provides significant improvement in damping the load oscillations by both reducing the maximum amplitude and damping its motion. This is more pronounced in the 6 m cable system, where elimination of the swing occurs within 20 seconds. For the 26 m configuration the swing control is not as good as in the other cases, with the controlled swinging remaining closer to the uncontrolled swinging; however, significant reduction is present. The simulations show that longer cables are harder to control, so it is recommended to use short cables whenever possible as they allow for faster swing reduction and even elimination.

As was mentioned earlier in this section, there is less swinging of the load when the going from hover to forward movement. This is the result of the drag force generated when in motion, which pushes the load and disrupts its pendulous behaviour. Once in hover, drag is reduced and the load behaves like a pendulum unless control action is applied, as can be seen when the LSC is not present.

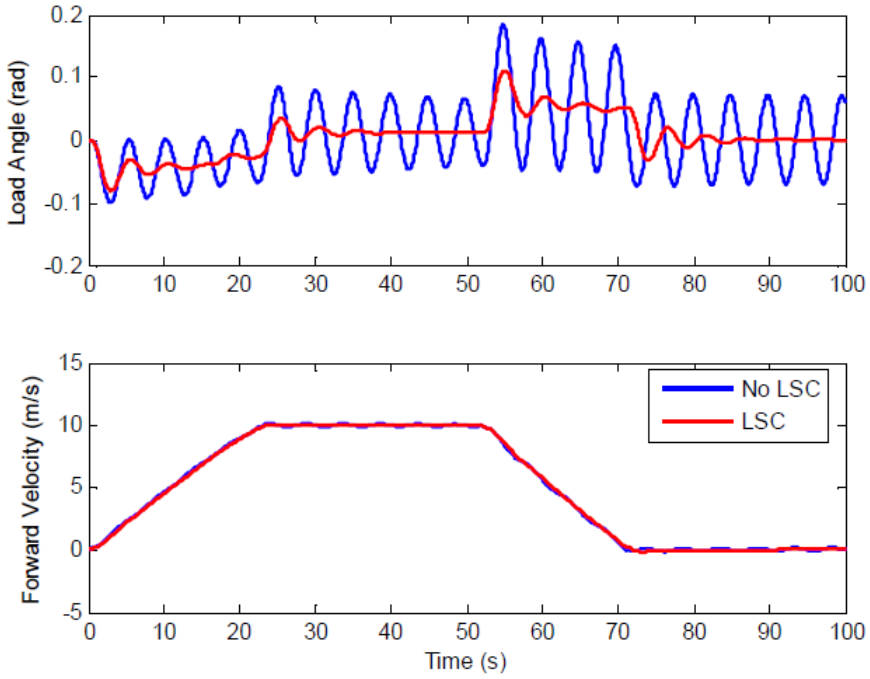

Figure 5-5 Effect on load and helicopter response to applying LSC with cable length of 6 m

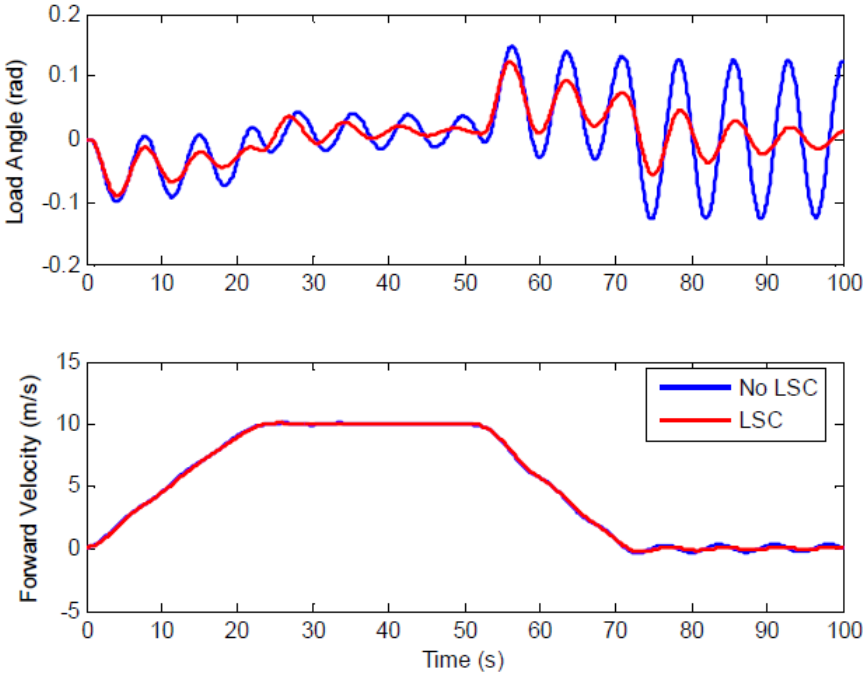

Figure 5-6 Effect on load and helicopter response to applying LSC with cable length of 13 m

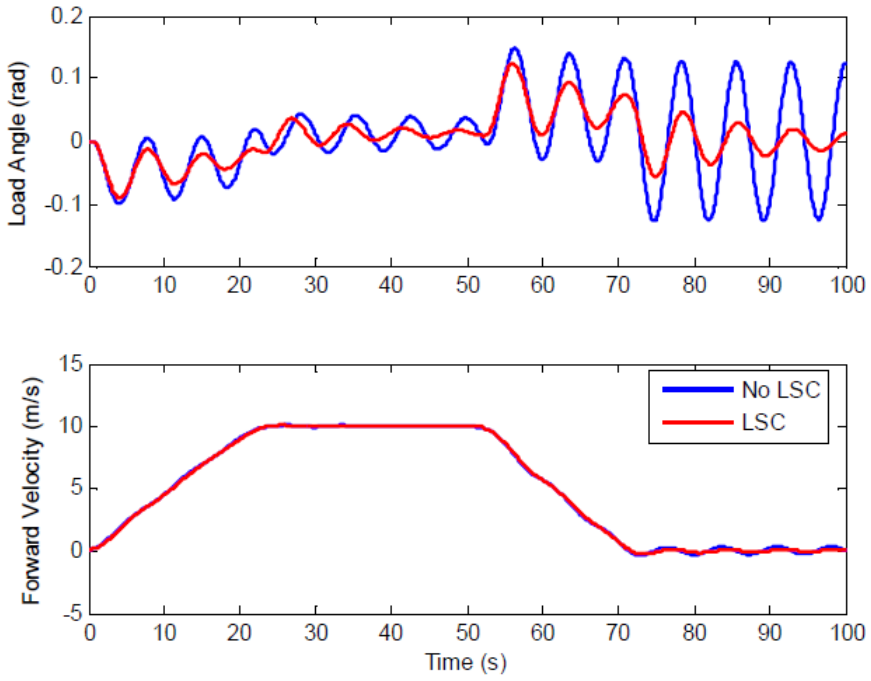

Figure 5-7 Effect on load and helicopter response to applying LSC with cable length of 26 m

It is important to remember that the application of the LSC term affects the helicopter behaviour as it does not consider the mismatch error between the helicopter and the ideal model. Because of that, it is necessary to check how the helicopter behaviour compares to the target behaviour. ADS-33 states that any residual oscillation greater than 0.5 deg (0.01 rad) will be deemed excessive, so it is desired that the deviation from the ideal model be less than 0.01 rad. The comparison of pitch attitude response to ideal response was realized for the same three cable length and mass configurations and can be seen in Figure 5-8 through Figure 5-10. The figures also present the control signals generated to achieve the pitch attitude, to verify that they are within the range defined in sections 5.1. The reference signal presented is the pitch attitude commands used to obtain the velocity shown in Figure 5-5 through Figure 5-7.

A clear deviation of the pitch attitude from the target response can be seen in the three cases. The 6 m cable configuration is the only one to surpass the allowed 0.01 rad deviation. This however, is not sustained as the pitch attitude is back within the acceptable range after 5 s. The other two configurations remain within 0.01 rad for the duration of the simulation, with the 26 m cable system always within 0.004 rad of the desired value. The deviation, resulting from corrections to reduce load oscillation, does not produce a serious impact on the helicopter response. The control signals generated remain small and within the acceptable range defined by the saturation limits.

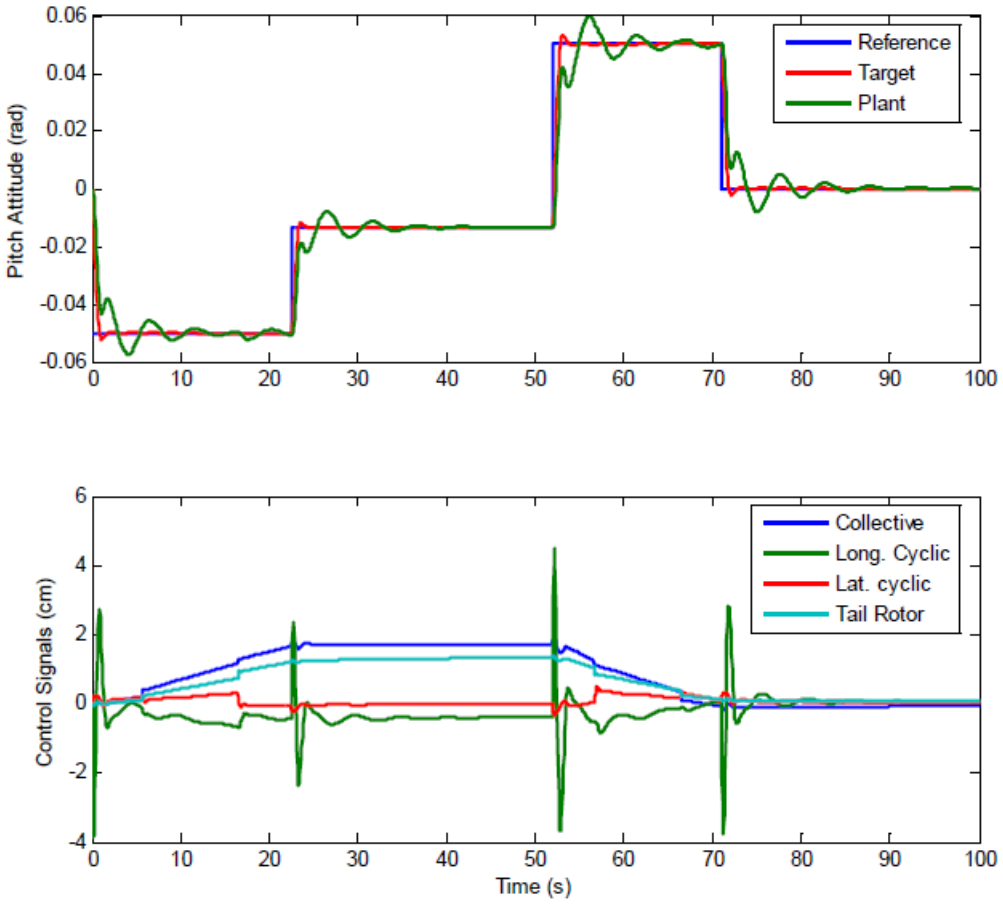

Figure 5-8 Pitch attitude response and control signals for cable length of 6 m

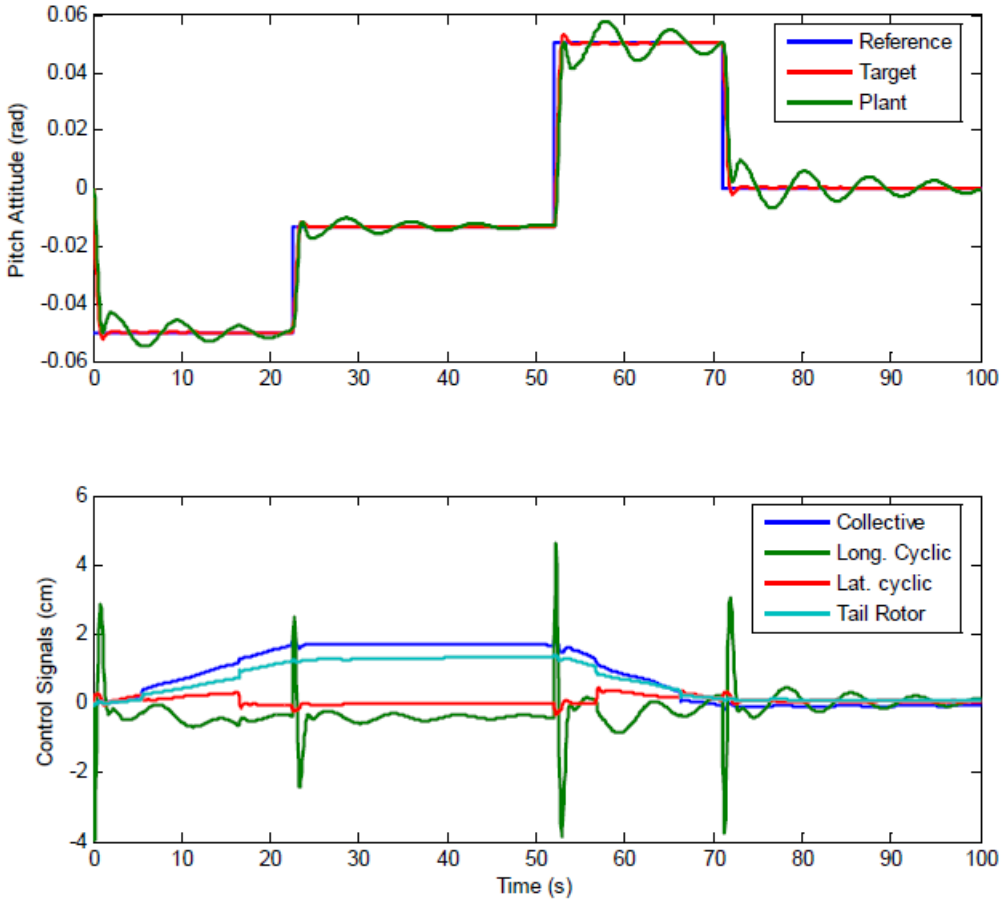

Figure 5-9 Pitch attitude response and control signals for cable length of 13 m

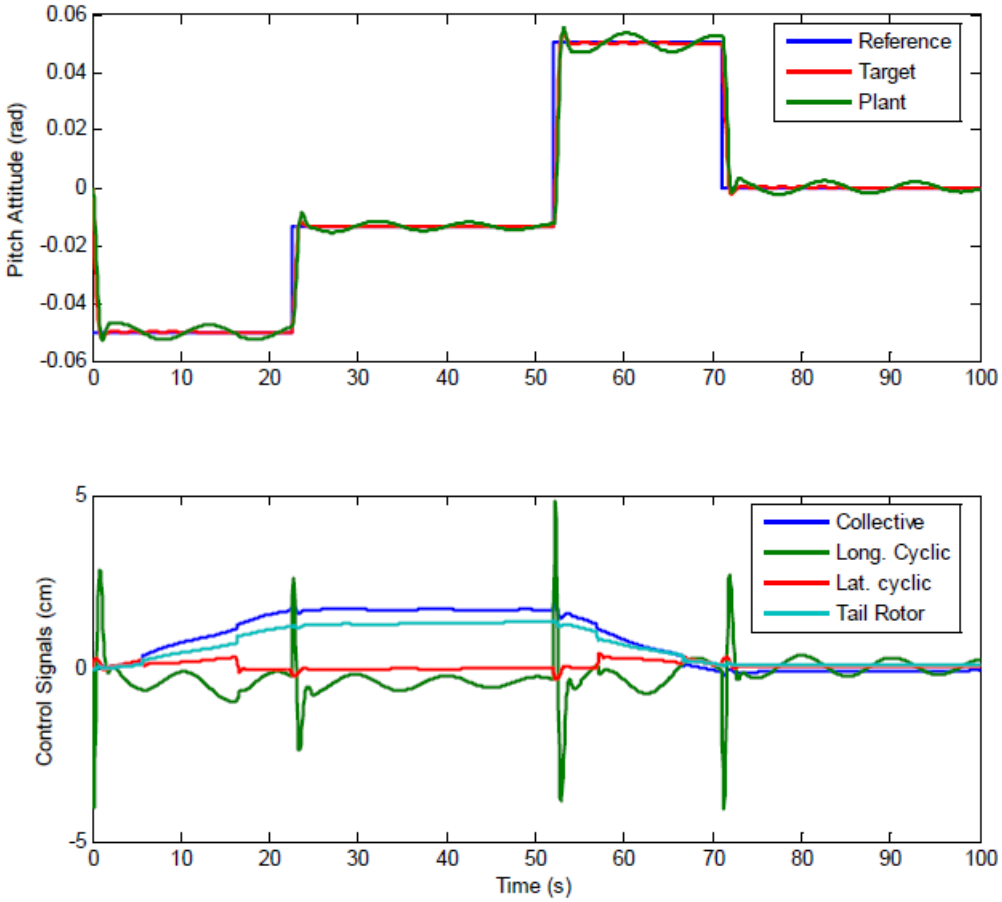

Figure 5-10 Pitch attitude response and control signals cable length of 26 m

Chapter 6 Conclusions

6.1 Summary

This thesis proposes a controller designed to follow human generated commands, rather than create its own, to arrive at a given location. It is intended to be a stability augmentation system that makes corrections, when needed, to help the pilot control the suspended load. This is accomplished through the synthesis of a model following controller that mimics an ideal model derived from the ADS-33 specified level 1 handling qualities. A load stability control (LSC) term is then added to the controller to dampen load oscillation.

Simulation results show that the addition of the LSC term improves the system behaviour by reducing load oscillation. The controller does two things to aid the pilot when flying with a slung load. First, it modifies the helicopter behaviour during the acceleration and stopping of the helicopter to prevent swinging of the load from taking place, or at least reduce the magnitude of the oscillations. The second thing is the corrective actions used to dampen the load oscillations if they take place.

Results also show that the LSC has little effect on the desired helicopter response with only a small deviation from the target behaviour. Only with short cables does this deviation exceed the allowed 0.01 rad; however, it is not a sustained oscillation. This

ensures that the aircraft will meet the level 1 handling qualities specified for helicopters traveling without a suspended load.

With respect to the cable length, it is recommended to avoid the 10 m to 19 m zone as the system presents fluctuating behaviour and large variations of load oscillation. Despite this, the proposed controller can still be used with any of the cables and will provide improvement in damping load oscillations.

6.2 Future work

Run a similar study using different helicopters to test how the controller responds with other helicopters.

While a two dimensional load model shows the longitudinal displacement of the load, which was the main concern of this study, a three dimensional model may provide better results concerning the overall motion of the load. This study did not investigate the lateral movement of the aircraft; however, this movement is essential during real flight manoeuvres as well as for stabilizing the load when load swinging occurs in this direction.

Helicopter behaviour is highly non-linear, and although this study used multiple trim conditions to approach the non-linear behaviour, more accurate and realistic simulation results can be obtained by using the non-linear model. After a successful non-

linear evaluation, the final measure to determine the controller's effectiveness would be to do real life experimental flight testing.

Bibliography

Abdul Kadir, H., Abd Wahab, M., Tomari, M., Shoiat@Ishak, M., & Hashim, H. (2009). Control of JIB model using PID and LQR optimization. *FKEE Compilation of Papers 2009 - VOLUME 2*, pp. 189-199.

Abdullah, J., Ruslee, R., & Jalani, J. (2011). Performance Comparison between LQR and FLC for Automatic 3 DOF Crane Systems. *International Journal of Control and Automation, 4*(4), pp. 163-178.

Adams, C. (2012). *Modeling and Control of Helicopters Carrying Suspended Loads.* Atlanta, GA: Georgia institute of technology.

Adeli, M.; Zarabadipour, H.; Aliyari Shoorehdeli, M. (2011). Crane Control Via Parallel Distributed Fuzzy LQR Controller Using Genetic Fuzzy Rule Selection. *2nd International Conference on Control, Instrumentation and Automation*, pp. 390-395. Shiraz, Iran.

(2000). *Aeronautical Design Standard, Performance Specification, Handling Qualities Requirements for Military Rotorcraft.* United States Army Aviation and, Redtone Arsenal, AL.

Ahmad, M., Ramli, M., Raja Ismail, R., Samin, R., & Zawawi, M. (2010). Implementation of Input Shaping in Hybrid Control Schemes of a Lab-scaled Rotary Crane System. *2010 IEEE International Conference on Industrial Technology (ICIT)*, pp. 530-534. Viña del Mar, Chile.

Ahmad, M., Samin, R., & Zawawi, M. (2010). Comparison of Optimal and Intelligent Sway Control for a Lab-Scale Rotary Crane System. *Second International*

Conference on Computer Engineering and Applications, pp. 229 - 234 vol. 1. Bali Island, Indonesia.

Air BP. (2012). Retrieved from Avgas vs Jet Fuel: http://www.bp.com/sectiongenericarticle.do?categoryId=4503818&contentId=57639

Alsop, C., Forster, G., & Holmes, F. (1965). Ore unloader automation - a fesability study. *IFAC Workshop on System Engineering for Control Systems*, pp. 295-305. Tokyo, Japan.

Asseo, & Sabi, J. (1971). *Feasibility of Using Active Winch Controllers for Sling-Load Stabilization in Heavy Lift Helicopters.* Cornell Aeronaut. Lab., Inc.

Astrom, K. J., & Wittenmark, B. (1990). *Computer Controlled Systems.* New Jersey: Prentice.

AutoCopter. (2011, October 10). *Products*. Retrieved from Autocopter: http://www.autocopter.us/product.htm

Balmford, D., & Done, G. (2000). *Bramwell's Helicopter Dynamics* (2nd ed.). Burlington, MA: Elsevier Science & Technology.

Bernard, M., Kondak, K., & Hommel, G. (2008). A Slung Load Transportation System Based on Small Size Helicopters. *Autonomous Systems – Self-Organization, Management, and Control*, pp. 49-61.

Bisgaard, M. (2008). *Modeling, estimation, and control of helicopter slung load system.* PhD thesis, Aalborg University.

Burananda, A., Ngamwiwit, J., Panaudomsup, S., Benjanarasuth, T., & Komine, N. (2002). Neural network based self-tuning control for overhead crane systems. *41st SICE Annual Conference: SICE 2002*, pp. 1944 - 1947 vol.3. Osaka, Japan.

Canadian Air-Crane Ltd. (2012). Retrieved from Mining: http://www.air-crane.com/services/mining.html

Canadian Air-Crane Ltd. (2012). Retrieved from Oil & Gas: http://www.air-crane.com/services/oil_gas.html

Cheetham, J. L., & Buckingham, A. J. (1998). *Aircraft Accident Report.* Civil Aviation Authority of New Zealand.

Chih-Hui, C., & Chun-Hsien, L. (2010). Adaptive output recurrent neural network for overhead crane system. *SICE Annual Conference 2010*, pp. 1082 - 1087. Taipei, Taiwan.

Cicolani, L. S., & Ehlers, G. E. (2002). Modeling and Simulation of a Helicopter Slung Load Stabilization Device. *American Helicopter Society 58th Annual Forum*, pp. 2346-2357. Montreal, Canada.

Cicolani, L. S., & Kannin, G. (1992). *Equations of Motion of Slung-Load Systems, Including Multilift Systems.* TP- 3280, NASA .

Cicolani, L. S., Kanning, G., & Synnestvedt, R. (1995). Simulation of the dynamics of helicopter slung load systems. *American Helicopter Society, 40*, pp. 44-61.

Conklin & de Decker Associates, Inc. (2012). Retrieved from Aircraft Cost Summary: https://www.conklindd.com/CDALibrary/ACCostSummary.aspx

Conklin & de Decker Associates, Inc. (2012). Retrieved from Aircraft Variable Costs: https://www.conklindd.com/Page.aspx?cid=1115

Construction Helicopters Incorporated. (2008). Retrieved from Construction Services: http://www.constructionhelicopters.com/construction.html

Cooper, G. E., & Harper Jr., R. P. (1969). *The Use of Pilot Ratings in the Evaluation of Aircraft Handling Qualities.* NASA.

Crane, D. (2006, February 17). *Exclusive Video: Unmanned Mini-Helicopter Gets 'Weaponized' with AA-12 Shotgun*. Retrieved from Defense Review: http://www.defensereview.com/exclusive-video-unmanned-mini-helicopter-gets-weaponized-with-aa-12-shotgun/

Dadone, P., & VanLandingham, H. (2001). Load transfer control for a gantry crane with arbitrary delay constraints. *Journal of Vibration and Control,* 8(2) , pp. 135-158.

Faille, D., & Van der Weiden, A. (1995). Robust Regulation of a Flying Crane. *4th IEEE Conference on Control Applications,* pp. 494 - 499. Albany, NY.

Garrido, S., Abderrahim, M., Gimenez, A., & Balaguer, C. (2008). Anti-Swinging Input Shaping Control of an Automatic Construction Crane. *IEEE Transactions on Automation Science and Engineering,* 5(3), pp. 549 - 557.

Gera, J., & Farmer, J. S. (1974). *A Method of Automatically Stabilizing Helicopter Sling Loads.* NASA .

Gupta, N. K., & Bryson, J. A. (1973). *Automatic Control of a Helicopter With a Hanging Load.* Department of Aeronautics and Astronautics, Stanford University, Stanford, California.

Hazlerigg, A. (1972). Automatic control of crane operations. *IFAC 5th World Congres Vol. 1*, Paper no. 11.3. Paris, France.

Heffley, R. F., Jewell, W. F., Lehman, J. M., & Van Winkle, R. A. (1979). *A Compilation and Analysis of Helicopter Handling Qualities Data.* NASA.

(2006). *Helicopter External Load Operations.* Civil Aviation Authority, Great Britain. Civil Aviation Authority, Great Britain.

Isaev, S. A., & Sumovskii, N. A. (1997). Resistance Reduction and Stability Improvement for Helicopter-Shipped Loads When a Leading Separation Zone is Organized. *Journal of Engineering Physics and Thermophysics, 70*(6), pp. 952-957.

Itoh, O., Migita, H., Itoh, J., & Irie, Y. (1993). Application of fuzzy control to automatic crane operation. *International Conference on Industrial Electronics, Control, and Instrumentation*, pp. 161 - 164 vol.1. Maui, HI.

Jones, J., & Petterson, B. (1988). Oscillation damped movement of suspended objects. *IEEE International Conference on Robotics and Automation*, pp. 956-962. Philadelphia, PA.

Kim, M., & Kang, G. (1993). Design of Fuzzy Controller Based on Fuzzy Model for Container Crane System. *5th International Fuzzy Systems Association World Congres*, pp. 1250-1253 vol. 2. Seoul, South Korea.

Kuntze, H., & Strobel, H. (1975). A contribution to adaptive time-optimal crane control. *IFAC 6th World Congress Vol. 3*, Paper no. 4.5. Boston, MA.

Mendez, J., Acosta, L., Moreno, L., Hamilton, A., & Marichal, G. (1998). Design of a neural network based self-tuning controller for an overhead crane. *1998 IEEE International Conference on Control Applications*, pp. 168 - 171 vol.1. Trieste, Italy.

Moustafa, K., Ismail, M., Gad, E., & El-Moneer, A. (2006). Fuzzy control of flexible cable overhead cranes with load hoisting. *Transactions of the Institute of Measurement and Control, 28*(4), pp. 371-386.

(1997). *Multiservice Helicopter Sling Load: Basic Operations and Equipment.* Headquarters, Department of the Army, Department of the Air Force, Department of the Navy, Department of Transportation, Washington D.C.

Omar, H. M. (2009). New Fuzzy-Based Anti-Swing Controller for Helicopter Slung-Load System near Hover. *Computational Intelligence in Robotics and Automation*, pp. 474 - 479. Daejeon.

Ottander, J., & Johnson, E. (2010). Precision slung cargo delivery onto a moving platform. *AIAA Modeling and Simulation Technologies Conference*, pp. 2-5. Toronto, Canada.

Padfield, G. D. (2007). *Helicopter Flight dynamics* (2nd ed.). Blackwell Publishing.

Pardue, M. D., & Shaughnessy, J. D. (1979). *Design and Analysis of an Active Jet Control System for Helicopter Sling Loads.* Technical Paper, NASA.

Parny, R. (1993). Helicopter airborne services live line work. *In Proceedings of the 6th International Conference on Transmission and Distribution Construction and Live Line Maintenance,* pp. 74 – 87. Las Vegas, Navada: IEEE.

Potter, J., Singhose, W., & Costello, M. (2011). Reducing swing of model helicopter sling load using input shaping. *9th IEEE International Conference on Control and Automation*, pp. 348-353. Santiago, Chile.

Rachkov, M., Marques, L., & De Almeida, A. (2007). Stochastic control of helicopter suspended load position. *Mathematical and Computer Modelling of Dynamical Systems, 13*(2), pp. 115-124.

Seddon, J., & Newman, S. (2002). *Basic Helicopter Aerodynamics* (2nd ed.). Blackwell Publishing.

Shaughnessy, J. D., & Pardue, M. D. (1977). *Helicopter Sling Load Accident/Incident Survey.* Technical Memorandum, NASA.

Siegwart, R., & Nourbakhsh, I. (2004). *Introduction to Autonomous Mobile Robots.* Cambridge, Massachusetts: Massachusetts Institute of Technology.

Smith, J. H., Allen, G. M., & Vensel, D. (1973). *Design, Fabrication, and Flight Test of the Active Arm External Load Stabilization System for Cargo Handling Helicopters.* Boeing Vertol Company.

Stevens, B. L., & Lewis, F. L. (1992). *Aircraft Control and Simulation.* New York: Wiley-Intescience.

Stuckey, R. (2001). *Mathematical Modelling of Helicopter Slung-Load Systems.* Air Operations Division Aeronautical and Maritime Research Laboratory, Fishermans Bend, Victoria, Australia.

Szuladzinski, G. (2009). Formulas for Mechanical and Structural Shock and Impact. *CRC Press*, pp. 747–748.

Thalapil, J. (2012). Input Shaping for Sway Control in Gantry Cranes. *IOSR Journal of Mechanical and Civil Engineering,* 1(2), pp. 36-46.

Thanapalan, K. (2010). Modelling of A Helicopter System. *1st Virtual Control Conference.* Denmark.

Thanapalan, K., & Wong, T. M. (2010). Modeling of a Helicopter with an Under-Slung Load System. *29th Chinese Control Conference*, pp. 1451 - 1456. Beijing, China.

Trentini, M. (1999). *Mixed Norm Control of a Helicopter.* Ph.D. dissertation, Univ. of Calgary, Calgary, AB.

Tsitsilonis, L., & McLean, D. (1981). Station-keeping control system for a helicopter with a suspended load. *Transactions of the Institute of Measurement and Control, 3*(3), pp. 121-135.

Vaha, P., & Marttinen, A. (1989). Conventional and optimal control in swing-free transfer of suspended load. *IEEE International Conference on Control and Applications: ICCON 89,* pp. 387 - 391. Jerusalem, Israel.

Veillette, P. R. (1999). External Loads, Power Plants Problems and Obstacles Challenge Pilots During Aerial Fire Fighting Operation. *Flight Safety Foundation, 25*(6).

Wagtendonk, W. J. (2006). *Principles of helicopter Flight* (2nd ed.). Newcastle, WA: ASA.

Williams, R. L., & Lawrence, D. A. (2007). *Linear State-Space Control Systems.* Hobiken, New Jersey, USA: John Wiley & Sons, Inc.

Yamada, S., Fujikawa, H., & Matsumoto, K. (1983). Suboptimal control of the roof crane by using the microcomputer. *Conference on Industrial Electronics: IECON 83,* pp. 323-328. San Francisco, CA.

Yamada, S., Fujikawa, H., Takeuchi, O., & Wakasugi, Y. (1989). Fuzzy control of the roof crane. *15th Annual Conference of IEEE Industrial Electronics Society*, pp. 709 - 714 vol.4. Philadelphia, PA.

Yasunobu, S., & Hasegawa, T. (1986). Evaluation of an automatic container crane operation system based on predictive fuzzy control. *Control Theory and Advanced Technology, 2*(3), pp. 419-432.

Zawawi, M., Wan Zamani, W., Ahmad, M., Saealal, M., & Samin, R. (2011). Feedback Control Schemes for Gantry Crane System incorporating Payload. *2011 IEEE Symposium on Industrial Electronics and Applications: ISIEA2011*, pp. 370-375. Langkawi, Malaysia.

Appendix A Linearized Equations

In this appendix the linearized form of the equations derived in chapter 3 are presented.

For Equation (3.7)

$\ddot{\alpha} = \frac{1}{\frac{1}{6}mbh+ml^2}\left[-mgl(sin\theta cos\alpha + cos\theta sin\alpha) + C_U l sign(U_L){U_L}^2 cos\alpha -\right.$

$\left. CWlsignWLWL2sin\alpha\right.$

the partial derivatives evaluated at the nominal operating point are as follows

$$\frac{\partial\ddot{\alpha}}{\partial U} = \frac{1}{\frac{1}{6}mbh + ml^2}\left[2C_d lcos(\tilde{\alpha})\left[\tilde{U} - lcos(\tilde{\alpha})\tilde{\dot{\alpha}}\right]\right]$$

$$\frac{\partial\ddot{\alpha}}{\partial W} = \frac{1}{\frac{1}{6}mbh + ml^2}\left[-2C_d lsin(\tilde{\alpha})\left[\tilde{W} - lsin(\tilde{\alpha})\tilde{\dot{\alpha}}\right]\right]$$

$$\frac{\partial\ddot{\alpha}}{\partial Q} = 0$$

$$\frac{\partial\ddot{\alpha}}{\partial V} = 0$$

$$\frac{\partial\ddot{\alpha}}{\partial P} = 0$$

$$\frac{\partial\ddot{\alpha}}{\partial R} = 0$$

$$\frac{\partial\ddot{\alpha}}{\partial \theta} = \frac{gl}{\frac{1}{6}bh + l^2}\left[sin(\tilde{\alpha})sin\left(\tilde{\theta}\right) - cos(\tilde{\alpha})cos\left(\tilde{\theta}\right)\right]$$

$$\frac{\partial\ddot{\alpha}}{\partial \varphi} = 0$$

$$\frac{\partial \ddot{\alpha}}{\partial \alpha} = \frac{1}{\frac{1}{6}mbh + ml^2}\Big\{mgl\left(sin(\tilde{\alpha})sin(\tilde{\theta}) - cos(\tilde{\alpha})cos(\tilde{\theta})\right)$$

$$+ C_d l sin(\tilde{\alpha})\left[2l\left[\widetilde{U} - lcos(\tilde{\alpha})\tilde{\dot{\alpha}}\right]\left(cos(\tilde{\alpha})\tilde{\dot{\alpha}}\right) - \left[\widetilde{U} - lcos(\tilde{\alpha})\tilde{\dot{\alpha}}\right]^2\right]$$

$$+ C_d l cos(\tilde{\alpha})\left[2l\left[\widetilde{W} - lsin(\tilde{\alpha})\tilde{\dot{\alpha}}\right]\left(sin(\tilde{\alpha})\tilde{\dot{\alpha}}\right) - \left[\widetilde{W} - lsin(\tilde{\alpha})\tilde{\dot{\alpha}}\right]^2\right]\Big\}$$

$$\frac{\partial \ddot{\alpha}}{\partial \dot{\alpha}} = \frac{1}{\frac{1}{6}mbh + ml^2}\left\{-2C_d l^2 cos^2(\tilde{\alpha})\left[\widetilde{U} - lcos(\tilde{\alpha})\tilde{\dot{\alpha}}\right] + 2C_d l^2 sin^2(\tilde{\alpha})\left[\widetilde{W} - lsin(\tilde{\alpha})\tilde{\dot{\alpha}}\right]\right\}$$

$$\frac{\partial \ddot{\alpha}}{\partial \delta_C} = 0$$

$$\frac{\partial \ddot{\alpha}}{\partial \delta_B} = 0$$

$$\frac{\partial \ddot{\alpha}}{\partial \delta_A} = 0$$

$$\frac{\partial \ddot{\alpha}}{\partial \delta_P} = 0$$

For Equation (3.13)

$$\dot{U} = \frac{M}{M+m}\dot{U}_H - \frac{1}{M+m}\left[ml(sin\alpha\dot{\alpha}^2 - cos\alpha\ddot{\alpha}) + C_U sign(U_L){U_L}^2 - mgsin\theta\right]$$

the partial derivatives evaluated at the nominal operating point are as follows

$$\frac{\partial \dot{U}}{\partial U} = \frac{M}{M+m}\frac{\partial \dot{U}_H}{\partial U} - \frac{1}{M+m}\left[-mlcos(\tilde{\alpha})\frac{\partial \ddot{\alpha}}{\partial U} + 2C_d\left[\widetilde{U} - lcos(\tilde{\alpha})\tilde{\dot{\alpha}}\right]\right]$$

$$\frac{\partial \dot{U}}{\partial W} = \frac{M}{M+m}\frac{\partial \dot{U}_H}{\partial W} - \frac{1}{M+m}\left[-mlcos(\tilde{\alpha})\frac{\partial \ddot{\alpha}}{\partial W}\right]$$

$$\frac{\partial \dot{U}}{\partial Q} = \frac{M}{M+m}\frac{\partial \dot{U}_H}{\partial Q}$$

$$\frac{\partial \dot{U}}{\partial V} = \frac{M}{M+m}\frac{\partial \dot{U}_H}{\partial V}$$

$$\frac{\partial \dot{U}}{\partial P} = \frac{M}{M+m}\frac{\partial \dot{U}_H}{\partial P}$$

$$\frac{\partial \dot{U}}{\partial R} = \frac{M}{M+m}\frac{\partial \dot{U}_H}{\partial R}$$

$$\frac{\partial \dot{U}}{\partial \theta} = \frac{M}{M+m}\frac{\partial \dot{U}_H}{\partial \theta} - \frac{1}{M+m}\left[-mlcos(\tilde{\alpha})\frac{\partial \ddot{\alpha}}{\partial \theta} - mgcos(\tilde{\theta})\right]$$

$$\frac{\partial \dot{U}}{\partial \varphi} = \frac{M}{M+m}\frac{\partial \dot{U}_H}{\partial \varphi}$$

$$\frac{\partial \dot{U}}{\partial \alpha} = -\frac{1}{M+m}\left\{ml\left[sin(\tilde{\alpha})\tilde{\ddot{\alpha}} - cos(\tilde{\alpha})\frac{\partial \ddot{\alpha}}{\partial \alpha} + cos(\tilde{\alpha})\tilde{\dot{\alpha}}^2\right]\right.$$

$$\left. + 2C_d l\left(sin(\tilde{\alpha})\tilde{\dot{\alpha}}\right)\left[\tilde{U} - lcos(\tilde{\alpha})\tilde{\dot{\alpha}}\right]\right\}$$

$$\frac{\partial \dot{U}}{\partial \dot{\alpha}} = -\frac{1}{M+m}\left\{ml\left[2sin(\tilde{\alpha})\tilde{\dot{\alpha}} - cos(\tilde{\alpha})\frac{\partial \ddot{\alpha}}{\partial \dot{\alpha}}\right] + 2C_d lcos(\tilde{\alpha})\left[\tilde{U} - lcos(\tilde{\alpha})\tilde{\dot{\alpha}}\right]\right\}$$

$$\frac{\partial \dot{U}}{\partial \delta_C} = \frac{M}{M+m}\frac{\partial \dot{U}_H}{\partial \delta_C}$$

$$\frac{\partial \dot{U}}{\partial \delta_B} = \frac{M}{M+m}\frac{\partial \dot{U}_H}{\partial \delta_B}$$

$$\frac{\partial \dot{U}}{\partial \delta_A} = \frac{M}{M+m}\frac{\partial \dot{U}_H}{\partial \delta_B}$$

$$\frac{\partial \dot{U}}{\partial \delta_P} = \frac{M}{M+m}\frac{\partial \dot{U}_H}{\partial \delta_P}$$

For Equation (3.14)

$$\dot{W} = \frac{M}{M+m}\dot{W}_H + \frac{1}{M+m}\left[ml(cos\alpha\dot{\alpha}^2 + sin\alpha\ddot{\alpha}) + C_W sign(W_L){W_L}^2 + mgcos\theta\right]$$

the partial derivatives evaluated at the nominal operating point are as follows

$$\frac{\partial \dot{W}}{\partial U} = \frac{M}{M+m}\frac{\partial \dot{W}_H}{\partial U} + \frac{1}{M+m}\left[mlsin(\tilde{\alpha})\frac{\partial \ddot{\alpha}}{\partial U}\right]$$

$$\frac{\partial \dot{W}}{\partial W} = \frac{M}{M+m}\frac{\partial \dot{W}_H}{\partial W} + \frac{1}{M+m}\left[mlsin(\tilde{\alpha})\frac{\partial \ddot{\alpha}}{\partial W} + 2C_d\left[\widetilde{W} - lsin(\tilde{\alpha})\tilde{\dot{\alpha}}\right]\right]$$

$$\frac{\partial \dot{W}}{\partial Q} = \frac{M}{M+m}\frac{\partial \dot{W}_H}{\partial Q}$$

$$\frac{\partial \dot{W}}{\partial V} = \frac{M}{M+m}\frac{\partial \dot{W}_H}{\partial V}$$

$$\frac{\partial \dot{W}}{\partial P} = \frac{M}{M+m}\frac{\partial \dot{W}_H}{\partial P}$$

$$\frac{\partial \dot{W}}{\partial R} = \frac{M}{M+m}\frac{\partial \dot{W}_H}{\partial R}$$

$$\frac{\partial \dot{W}}{\partial \theta} = \frac{M}{M+m}\frac{\partial \dot{W}_H}{\partial \theta} + \frac{1}{M+m}\left[mlsin(\tilde{\alpha})\frac{\partial \ddot{\alpha}}{\partial \theta} - mgsin(\tilde{\theta})\right]$$

$$\frac{\partial \dot{W}}{\partial \varphi} = \frac{M}{M+m}\frac{\partial \dot{W}_H}{\partial \varphi}$$

$$\frac{\partial \dot{W}}{\partial \alpha} = \frac{1}{M+m}\left\{ml\left[cos(\tilde{\alpha})\tilde{\ddot{\alpha}} + sin(\tilde{\alpha})\frac{\partial \ddot{\alpha}}{\partial \alpha} - sin(\tilde{\alpha})\tilde{\dot{\alpha}}^2\right]\right.$$
$$\left. - 2C_d l\left(cos(\tilde{\alpha})\tilde{\dot{\alpha}}\right)\left[\widetilde{W} - lsin(\tilde{\alpha})\tilde{\dot{\alpha}}\right]\right\}$$

$$\frac{\partial \dot{W}}{\partial \dot{\alpha}} = \frac{1}{M+m}\left\{ml\left[2cos(\tilde{\alpha})\tilde{\dot{\alpha}} + sin(\tilde{\alpha})\frac{\partial \ddot{\alpha}}{\partial \dot{\alpha}}\right] - 2C_d lsin(\tilde{\alpha})\left[\widetilde{W} - lsin(\tilde{\alpha})\tilde{\dot{\alpha}}\right]\right\}$$

$$\frac{\partial \dot{W}}{\partial \delta_C} = \frac{M}{M+m}\frac{\partial \dot{W}_H}{\partial \delta_C}$$

$$\frac{\partial \dot{W}}{\partial \delta_B} = \frac{M}{M+m}\frac{\partial \dot{W}_H}{\partial \delta_B}$$

$$\frac{\partial \dot{W}}{\partial \delta_A} = \frac{M}{M+m}\frac{\partial \dot{W}_H}{\partial \delta_A}$$

$$\frac{\partial \dot{W}}{\partial \delta_P} = \frac{M}{M+m}\frac{\partial \dot{W}_H}{\partial \delta_P}$$

For Equation (3.15)

$$\dot{Q} = \dot{Q}_H - \frac{z_{cg}}{I_y}\left[m\left(\dot{U} - l(cos\alpha\ddot{\alpha} - sin\alpha\dot{\alpha}^2)\right) + C_U sign(U_L){U_L}^2 - mgsin\theta\right]$$

the partial derivatives evaluated at the nominal operating point are as follows

$$\frac{\partial \dot{Q}}{\partial U} = \frac{\partial \dot{Q}_H}{\partial U} - \frac{z_{cg}}{I_y}\left[m\left(\frac{\partial \dot{U}}{\partial U} - lcos(\tilde{\alpha})\frac{\partial \ddot{\alpha}}{\partial U}\right) + 2C_d\left[\tilde{U} - lcos(\tilde{\alpha})\tilde{\dot{\alpha}}\right]\right]$$

$$\frac{\partial \dot{Q}}{\partial W} = \frac{\partial \dot{Q}_H}{\partial W} - \frac{z_{cg}}{I_y}\left[m\left(\frac{\partial \dot{U}}{\partial W} - lcos(\tilde{\alpha})\frac{\partial \ddot{\alpha}}{\partial W}\right)\right]$$

$$\frac{\partial \dot{Q}}{\partial Q} = \frac{\partial \dot{Q}_H}{\partial Q} - \frac{z_{cg}}{I_y}\left(\frac{\partial \dot{U}}{\partial Q}\right)$$

$$\frac{\partial \dot{Q}}{\partial V} = \frac{\partial \dot{Q}_H}{\partial V} - \frac{z_{cg}}{I_y}\left(\frac{\partial \dot{U}}{\partial V}\right)$$

$$\frac{\partial \dot{Q}}{\partial P} = \frac{\partial \dot{Q}_H}{\partial P} - \frac{z_{cg}}{I_y}\left(\frac{\partial \dot{U}}{\partial P}\right)$$

$$\frac{\partial \dot{Q}}{\partial R} = \frac{\partial \dot{Q}_H}{\partial R} - \frac{z_{cg}}{I_y}\left(\frac{\partial \dot{U}}{\partial R}\right)$$

$$\frac{\partial \dot{Q}}{\partial \theta} = \frac{\partial \dot{Q}_H}{\partial \theta} - \frac{z_{cg}}{I_y}\left[m\left(\frac{\partial \dot{U}}{\partial \theta} - lcos(\tilde{\alpha})\frac{\partial \ddot{\alpha}}{\partial U}\right) + mgcos(\tilde{\theta})\right]$$

$$\frac{\partial \dot{Q}}{\partial \varphi} = \frac{\partial \dot{Q}_H}{\partial \varphi} - \frac{z_{cg}}{I_y}\left(\frac{\partial \dot{U}}{\partial \varphi}\right)$$

$$\frac{\partial \dot{Q}}{\partial \alpha} = -\frac{z_{cg}}{I_y}\left\{ m\left[\frac{\partial \dot{U}}{\partial \alpha} + l\left(sin(\tilde{\alpha})\tilde{\ddot{\alpha}} - cos(\tilde{\alpha})\frac{\partial \ddot{\alpha}}{\partial \alpha} + cos(\tilde{\alpha})\tilde{\dot{\alpha}}^2\right)\right]\right.$$

$$\left. + 2C_d l\left(sin(\tilde{\alpha})\tilde{\dot{\alpha}}\right)\left[\tilde{U} - lcos(\tilde{\alpha})\tilde{\dot{\alpha}}\right]\right\}$$

$$\frac{\partial \dot{Q}}{\partial \dot{\alpha}} = -\frac{z_{cg}}{I_y}\left\{m\left[\frac{\partial \dot{U}}{\partial \dot{\alpha}} + l\left(2sin(\tilde{\alpha})\tilde{\dot{\alpha}} - cos(\tilde{\alpha})\frac{\partial \ddot{\alpha}}{\partial \dot{\alpha}}\right)\right] - 2C_d lcos(\tilde{\alpha})\left[\tilde{U} - lcos(\tilde{\alpha})\tilde{\dot{\alpha}}\right]\right\}$$

$$\frac{\partial \dot{Q}}{\partial \delta_C} = \frac{\partial \dot{Q}_H}{\partial \delta_C} - \frac{z_{cg}}{I_y}\left(\frac{\partial \dot{U}}{\partial \delta_C}\right)$$

$$\frac{\partial \dot{Q}}{\partial \delta_B} = \frac{\partial \dot{Q}_H}{\partial \delta_B} - \frac{z_{cg}}{I_y}\left(\frac{\partial \dot{U}}{\partial \delta_B}\right)$$

$$\frac{\partial \dot{Q}}{\partial \delta_A} = \frac{\partial \dot{Q}_H}{\partial \delta_A} - \frac{z_{cg}}{I_y}\left(\frac{\partial \dot{U}}{\partial \delta_A}\right)$$

$$\frac{\partial \dot{Q}}{\partial \delta_P} = \frac{\partial \dot{Q}_H}{\partial \delta_P} - \frac{z_{cg}}{I_y}\left(\frac{\partial \dot{U}}{\partial \delta_P}\right)$$

Appendix B Matlab Code

In this appendix the Matlab code and Simulink program used for the simulation results in Chapter 5 are presented.

Matlab code

```
clear

ww=4;
lsc=500;
cont=1;
m=500;

t1=22.5;
t2=52.5;
t3=70;
tf=100;

for l=26:-1:6

    % x=[ U ; forward velocity
    %     W ; vertical velocity
    %     Q ; pitch rate
    %     V ; lateral velocity
    %     P ; roll rate
    %     R ; yaw rate
    %     theta ; pitch attitude
    %     phi ; roll attitude
    %     alpha ; load angle
    %     alphadot ] ; load angle rate

    % u=[ deltac ; collective
    %     deltab ; longitudinal cyclic
    %     deltaa ; lateral cyclic
    %     deltap ] ; tail rotor

    %Ideal model

    lambdau=4.0 ;
    lambdaw=3.0 ;
    lambdav=4.0 ;
    lambdaR=5.0 ;
    Ctheta=0.7 ;
    wtheta=4.0 ;
    Cphi=0.7 ;
    wphi=4.0 ;
```

```
    lambdaalpha=3.0;

    Abar= [-lambdau 0 0 0 0 0 -lambdau 0 0 0 ;
            0 -lambdaw 0 0 0 0 0 0 0 0 ;
            0 0 -2*Ctheta*wtheta 0 0 0 -wtheta^2 0 0 0 ;
            0 0 0 -lambdav 0 0 0 lambdav 0 0 ;
            0 0 0 0 -2*Cphi*wphi 0 0 -wphi^2 0 0 ;
            0 0 0 0 0 -lambdaR 0 0 0 0 ;
            0 0 1 0 0 0 0 0 0 0 ;
            0 0 0 0 1 0 0 0 0 0 ;
            0 0 0 0 0 0 0 0 0 1 ;
           -lambdaalpha -lambdaalpha 0 0 0 0 0 0 -lambdaalpha -
lambdaalpha ];

    Bbar= [ 0 0 0 0 ;
            lambdaw 0 0 0 ;
            0 -wtheta^2 0 0 ;
            0 0 0 0 ;
            0 0 -wphi^2 0 ;
            0 0 0 lambdaR ;
            0 0 0 0 ;
            0 0 0 0 ;
            0 0 0 0 ;
            0 0 0 0 ] ;

    %hover

    A=[ -0.0034  0.0250  0.1767 -0.0077 -0.4225 -0.0777 -9.81 0 ;
        -0.0991 -0.3850  0.0888 -0.0982 -0.1209  0.6745  0    0 ;
         0.0062 -0.0124 -0.1900  0.0044  0.2342  0.0385  0    0 ;
         0.0150 -0.0040 -0.4071 -0.0451 -0.2670  0.2678  0    9.81 ;
         0.0253 -0.0162 -0.8779 -0.0417 -0.5720  0.1391  0    0 ;
        -0.0054 -0.0206 -0.0597  0.0687 -0.3176 -0.7094  0    0 ;
         0       0       1       0       0       0       0    0 ;
         0       0       0       0       1       0       0    0 ] ;

    B=[  0.0817  0.1249 -0.0009 -0.0007 ;
        -1.1729  0.0386  0.0036  0.0084 ;
        -0.0013 -0.0666  0.0004  0.0062 ;
        -0.0348  0.0017  0.1061  0.1959 ;
        -0.0443  0.0033  0.2217  0.1666 ;
         0.1718 -0.0004  0.0326 -0.4712 ;
         0       0       0       0 ;
         0       0       0       0 ] ;

    %nominal state values

    U0=0.51;
    V0=0;
    W0=0.04;
    P0=0;
    Q0=0;
    R0=0;
    alphadot0=0;
    count=0;
    while count<3
```

```
        % with suspended load

        Cd=1.1;     %drag coefficient
        rho=1.112;  %kg/m^3 air density at 90 kPa and 0°C
        S=1;        %m^2 surface area for U and W for cube
        m=m;        %kg load mass
        g=9.8;      %m/s^s gravitational acceleration
        l=l;        %m cable legnth
        l1=1.84;    %m vertical distance from cg to suspention point
        M=3629;     %kg helicopter nominal weight
        Ix=3966;    %kgm^2 moment of inertia about x axis
        Iy=14684;   %kgm^2 moment of inertia about y axis
        Ix=12541;   %kgm^2 moment of inertia about z axis
        kd=1/2*Cd*rho*S; %Proportionality constant of drag force

        syms theta0 phi0 alpha0 deltac0 deltab0 deltaa0 deltap0

        udot=
      M/(M+m)*(A(1,1)*U0+A(1,2)*W0+A(1,3)*Q0+A(1,4)*V0+A(1,5)*P0+A(1,6)
*R0+A(      1,7)*theta0+A(1,8)*phi0) +
      M/(M+m)*(B(1,1)*deltac0+B(1,2)*deltab0+B(1,3)*deltaa0+B(1,4)*delt
ap0) -            1/(M+m)*(m*l*(-cos(alpha0)* (( 1/(m*l)*(-
      m*g*(sin(theta0)*cos(alpha0)+cos(theta0)*sin(alpha0))+kd*sign(U0)
*U0^2*      cos(alpha0)-kd*sign(W0)*W0^2*sin(alpha0)) )) )
      +kd*sign(U0)*U0^2+m*g*sin(theta0)) ;

        wdot=
      M/(M+m)*(A(2,1)*U0+A(2,2)*W0+A(2,3)*Q0+A(2,4)*V0+A(2,5)*P0+A(2,6)
*R0+A(      2,7)*theta0+A(2,8)*phi0) +
      M/(M+m)*(B(2,1)*deltac0+B(2,2)*deltab0+B(2,3)*deltaa0+B(2,4)*delt
ap0) +      1/(M+m)*(m*l*(sin(alpha0)* ((
      1/(m*l)*(m*g*(sin(theta0)*cos(alpha0)+cos(theta0)*sin(alpha0))+kd
*sign(      U0)*U0^2*cos(alpha0)-kd*sign(W0)*W0^2*sin(alpha0)) )) )
      +kd*sign(W0)*W0^2+m*g*cos(theta0)) ;

        vdot=
      (A(4,1)*U0+A(4,2)*W0+A(4,3)*Q0+A(4,4)*V0+A(4,5)*P0+A(4,6)*R0+A(4,
7)*the      ta0+A(4,8)*phi0) +
      M/M*(B(4,1)*deltac0+B(4,2)*deltab0+B(4,3)*deltaa0+B(4,4)*deltap0)
;

        pdot=
      (A(5,1)*U0+A(5,2)*W0+A(5,3)*Q0+A(5,4)*V0+A(5,5)*P0+A(5,6)*R0+A(5,
7)*the      ta0+A(5,8)*phi0) +
      M/M*(B(5,1)*deltac0+B(5,2)*deltab0+B(5,3)*deltaa0+B(5,4)*deltap0)
;

        rdot=
      (A(6,1)*U0+A(6,2)*W0+A(6,3)*Q0+A(6,4)*V0+A(6,5)*P0+A(6,6)*R0+A(6,
7)*the      ta0+A(6,8)*phi0) +
      M/M*(B(6,1)*deltac0+B(6,2)*deltab0+B(6,3)*deltaa0+B(6,4)*deltap0)
;


        alphadotdot=
```

```
      1/(1/6*m*S^2+m*l^2)*l*(-
      m*g*(sin(theta0)*cos(alpha0)+cos(theta0)*sin(alpha0))+kd*sign(U0)
*U0^2*      cos(alpha0)-kd*sign(W0)*W0^2*sin(alpha0)) ;

        qdot=
      (A(3,1)*U0+A(3,2)*W0+A(3,3)*Q0+A(3,4)*V0+A(3,5)*P0+A(3,6)*R0+A(3,
7)*the      ta0+A(3,8)*phi0) +
      M/M*(B(3,1)*deltac0+B(3,2)*deltab0+B(3,3)*deltaa0+B(3,4)*deltap0)
+     l1*m/Iy* ((
      M/(M+m)*(A(1,1)*U0+A(1,2)*W0+A(1,3)*Q0+A(1,4)*V0+A(1,5)*P0+A(1,6)
*R0+A(      1,7)*theta0+A(1,8)*phi0) +
      M/(M+m)*(B(1,1)*deltac0+B(1,2)*deltab0+B(1,3)*deltaa0+B(1,4)*delt
ap0) -      1/(M+m)*(m*l*(-cos(alpha0)* (( 1/(m*l)*(-
      m*g*(sin(theta0)*cos(alpha0)+cos(theta0)*sin(alpha0))+kd*sign(U0)
*U0^2*      cos(alpha0)-kd*sign(W0)*W0^2*sin(alpha0)) )) )
      +kd*sign(U0)*U0^2+m*g*sin(theta0)) )) -l1/Iy*(-m*l*cos(alpha0)*
((
      1/(m*l)*(m*g*(sin(theta0)*cos(alpha0)-
      cos(theta0)*sin(alpha0))+kd*sign(U0)*U0^2*cos(alpha0)-
      kd*sign(W0)*W0^2*sin(alpha0))
))+kd*sign(U0)*U0^2+m*g*sin(theta0)) ;

        [alpha0, deltaa0, deltab0, deltac0, deltap0,
phi0,theta0]=solve(udot,            wdot, vdot, pdot, rdot,
            alphadotdot, qdot);

        alpha0=double(alpha0);
        deltaa0=double(deltaa0);
        deltab0=double(deltab0);
        deltac0=double(deltac0);
        deltap0=double(deltap0);
        phi0=double(phi0);
        theta0=double(theta0);

        alphadotdot=
      1/(1/6*m*S^2+m*l^2)*(-m*g*l*(-
      sin(theta0)*cos(alpha0)+cos(theta0)*sin(alpha0))+kd*(U0-
      l*cos(alpha0)*alphadot0)^2*l*cos(alpha0)-kd*(W0-
      l*sin(alpha0)*alphadot0)^2*l*sin(alpha0));

        %Expanded linear model

        A1=[ 0 0 0 0 0 0 0 0 0 0 ;
             0 0 0 0 0 0 0 0 0 0 ;
             0 0 0 0 0 0 0 0 0 0 ;
             A(4,1) A(4,2) A(4,3) A(4,4) A(4,5) A(4,6) A(4,7) A(4,8) 0
0 ;
             A(5,1) A(5,2) A(5,3) A(5,4) A(5,5) A(5,6) A(5,7) A(5,8) 0
0 ;
             A(6,1) A(6,2) A(6,3) A(6,4) A(6,5) A(6,6) A(6,7) A(6,8) 0
0 ;
             A(7,1) A(7,2) A(7,3) A(7,4) A(7,5) A(7,6) A(7,7) A(7,8) 0
0 ;
             A(8,1) A(8,2) A(8,3) A(8,4) A(8,5) A(8,6) A(8,7) A(8,8) 0
0 ;
             0 0 0 0 0 0 0 0 0 1 ;
```

```
          0 0 0 0 0 0 0 0 0 0 ] ;


        % alphadotdot

        A1(10,1)=1/(1/6*m*S^2+m*l^2)*(2*l*kd*cos(alpha0)*(U0-
                  l*cos(alpha0)*alphadot0)) ;
        A1(10,2)=1/(1/6*m*S^2+m*l^2)*(-2*l*kd*sin(alpha0)*(W0-
                  l*sin(alpha0)*alphadot0)) ;
        A1(10,3)=0 ;
        A1(10,4)=0 ;
        A1(10,5)=0 ;
        A1(10,6)=0 ;
        A1(10,7)=1/(1/6*m*S^2+m*l^2)*(m*g*l*(cos(alpha0)*cos(theta0)+
            sin(alpha0)*sin(theta0))) ;
        A1(10,8)=0 ;
        A1(10,9)=1/(1/6*m*S^2+m*l^2)*(m*g*l*(-sin(theta0)*sin(alpha0)-
            cos(theta0)*cos(alpha0))+kd*((U0-
                  l*cos(alpha0)*alphadot0)^2*(-sin(alpha0))+2*(U0-

      l*cos(alpha0)*alphadot0)*(l*sin(alpha0)*alphadot0)*cos(alpha0))-
            kd*((W0-l*sin(alpha0)*alphadot0)^2*cos(alpha0)+2*(W0-
                  l*sin(alpha0)*alphadot0)*(-
                        l*cos(alpha0)*alphadot0)*sin(alpha0))) ;
        A1(10,10)=1/(1/6*m*S^2+m*l^2)*l^2*(2*kd*(U0-
                  l*cos(alpha0)*alphadot0)*(-
            (cos(alpha0))^2)-2*kd*(W0-l*sin(alpha0)*alphadot0)*(-
                  (sin(alpha0))^2)) ;

        % Udot
        A1(1,1)=(M/(M+m))*(A(1,1)) - 1/(M+m)*(-
                  m*l*cos(alpha0)*A1(10,1)+kd*2*(U0-
            l*cos(alpha0)*alphadot0)) ;
        A1(1,2)=(M/(M+m))*(A(1,2)) - 1/(M+m)*(-
m*l*cos(alpha0)*A1(10,2)) ;
        A1(1,3)=(M/(M+m))*(A(1,3)) ;
        A1(1,4)=(M/(M+m))*(A(1,4)) ;
        A1(1,5)=(M/(M+m))*(A(1,5)) ;
        A1(1,6)=(M/(M+m))*(A(1,6)) ;
        A1(1,7)=(M/(M+m))*(A(1,7)) - 1/(M+m)*(-
                  m*l*cos(alpha0)*A1(10,7)+m*g*cos(theta0)) ;
        A1(1,8)=(M/(M+m))*(A(1,8)) ;
        A1(1,9)=-1/(M+m)*(m*l*(cos(alpha0)*alphadot0^2-
(cos(alpha0)*A1(10,9)-
            sin(alpha0)*alphadotdot)+2*kd*(U0-
                  l*cos(alpha0)*alphadot0)*(l*sin(alpha0)*alphadot0)))
;
        A1(1,10)=-1/(M+m)*(m*l*(2*sin(alpha0)*alphadot0-
                  cos(alpha0)*A1(10,10))+2*kd*(U0-
            l*cos(alpha0)*alphadot0)*(-l*cos(alpha0))) ;

        %Wdot
        A1(2,1)=(M/(M+m))*(A(2,1)) + 1/(M+m)*(m*l*sin(alpha0)*A1(10,1))
;
```

```
        A1(2,2)=(M/(M+m))*(A(2,2)) +
                  1/(M+m)*(m*l*sin(alpha0)*A1(10,2)+2*kd*(W0-
            l*sin(alpha0)*alphadot0)) ;
        A1(2,3)=(M/(M+m))*(A(2,3)) ;
        A1(2,4)=(M/(M+m))*(A(2,4)) ;
        A1(2,5)=(M/(M+m))*(A(2,5)) ;
        A1(2,6)=(M/(M+m))*(A(2,6)) ;
        A1(2,7)=(M/(M+m))*(A(2,7)) + 1/(M+m)*(m*l*sin(alpha0)*A1(10,7)-
                  m*g*sin(theta0)) ;
        A1(2,8)=(M/(M+m))*(A(2,8)) ;
        A1(2,9)=1/(M+m)*(m*l*(-
                  sin(alpha0)*alphadot0^2+(sin(alpha0)*A1(10,9)+
            cos(alpha0)*alphadotdot))+2*kd*(W0-
            l*alphadot0*sin(alpha0))*(-l*cos(alpha0)*alphadot0)) ;
        A1(2,10)=1/(M+m)*(m*l*(2*cos(alpha0)*alphadot0+sin(alpha0)
            *A1(10,10))+2*kd*(W0-l*alphadot0*sin(alpha0))*(-
l*sin(alpha0))) ;

        %Qdot
        A1(3,1)=A(3,1) - l1/Iy*(m*(A1(1,1)-l*(cos(alpha0)*A1(10,1)))
            +2*kd*(U0-l*cos(alpha0)*alphadot0)) ;
        A1(3,2)=A(3,2) - l1/Iy*(m*(A1(1,2)-l*cos(alpha0)*A1(10,2))) ;
        A1(3,3)=A(3,3) ;
        A1(3,4)=A(3,4) ;
        A1(3,5)=A(3,5) ;
        A1(3,6)=A(3,6) ;
        A1(3,7)=A(3,7) - l1/Iy*(m*(A1(1,7)-l*cos(alpha0)*A1(10,7))
            +m*g*cos(theta0)) ;
        A1(3,8)=A(3,8) ;
        A1(3,9)=-l1/Iy*(m*(A1(1,9)-l*(-cos(alpha0)*alphadot0^2
            +(cos(alpha0)*A1(10,9)-        sin(alpha0)*alphadotdot)))
            +2*kd*(U0-l*cos(alpha0)*alphadot0)*(l*sin(alpha0))) ;
        A1(3,10)=-l1/Iy*(m*(A1(1,10)-l*(-2*sin(alpha0)*alphadot0
            +cos(alpha0)*A1(10,10)))+2*kd*(U0-l*cos(alpha0)*alphadot0)
            *(-l*cos(alpha0))) ;

        B1=[(M/(M+m))*(B(1,1)) (M/(M+m))*(B(1,2)) (M/(M+m))*(B(1,3))
            (M/(M+m))*(B(1,4)) ;
            (M/(M+m))*(B(2,1)) (M/(M+m))*(B(2,2)) (M/(M+m))*(B(2,3))
            (M/(M+m))*(B(2,4)) ;
            B(3,1) B(3,2) B(3,3) B(3,4) ;
            B(4,1) B(4,2) B(4,3) B(4,4) ;
            B(5,1) B(5,2) B(5,3) B(5,4) ;
            B(6,1) B(6,2) B(6,3) B(6,4) ;
            B(7,1) B(7,2) B(7,3) B(7,4) ;
            B(8,1) B(8,2) B(8,3) B(8,4) ;
            0 0 0 0 ;
            0 0 0 0 ] ;

        B1(3,1)=B(3,1)-l1/Iy*(B1(1,1));
        B1(3,2)=B(3,2)-l1/Iy*(B1(1,2));
        B1(3,3)=B(3,3)-l1/Iy*(B1(1,3));
        B1(3,4)=B(3,4)-l1/Iy*(B1(1,4));

        H=[ 0 1 0 0 0 0 0 0 0 0 ;
            0 0 0 0 0 0 1 0 0 0 ;
```

```
    0 0 0 0 0 0 0 1 0 0 ;
    0 0 0 0 0 1 0 0 0 0 ];
Hbar=H;

[An,Am]=size(A1);
[Bn,Bm]=size(B1);

C=eye(An);
Cbar=C;

Aprime=[ A1 zeros(An,Am) ;
    zeros(An,Am) Abar ] ;
[Aprimen,Aprimem]=size(Aprime);

Bprime=[ B1 ;
    zeros(Bn,Bm) ] ;

Gprime=[ zeros(Bn,Bm) ;
    Bbar ] ;

Hprime=[ -H Hbar ] ;
[Hn,Hm]=size(Hprime);

F=zeros(Hn,Hn);
[Fn,Fm]=size(F);

Atilde=[ F Hprime ;
    zeros(Aprimen,Fm) Aprime ] ;
[Atn,Atm]=size(Atilde);

Btilde=[ zeros(Fn,Bm) ;
    Bprime ] ;



%controller design

Q=[ 10^ww 0 0 0 0 0 0 0 0 0 0 0 0 ;
    0 10^ww 0 0 0 0 0 0 0 0 0 0 0 ;
    0 0 10^ww 0 0 0 0 0 0 0 0 0 0 ;
    0 0 0 10^ww 0 0 0 0 0 0 0 0 0 ;
    0 0 0 0 0 0 0 0 0 0 0 0 0 ;
    0 0 0 0 0 0 0 0 0 0 0 0 0 ;
    0 0 0 0 0 0 0 0 0 0 0 0 0 ;
    0 0 0 0 0 0 0 0 0 0 0 0 0 ;
    0 0 0 0 0 0 0 0 0 0 0 0 0 ;
    0 0 0 0 0 0 0 0 0 0 0 0 0 ;
    0 0 0 0 0 0 0 0 0 0 0 0 0 ;
    0 0 0 0 0 0 0 0 0 0 0 0 0 ;
    0 0 0 0 0 0 0 0 0 0 0 0 0 cont*lsc ] ;

Q=[Q zeros(Atn-An,Am)];
Q=[Q ;
    zeros(An,Atm)] ;
```

```
R=[1/13.6^2 0 0 0 ;
    0 1/16.5^2 0 0 ;
    0 0 1/16.5^2 0 ;
    0 0 0 1/8.2^2 ] ;

[X2,L2,G1,r]=care(Atilde,Btilde,Q,R);
if count==0

    Ahover=Aprime;
    Bhover=Bprime;

    k1h=G1(:,1);

    for i=2:1:Hn
        k1h=[k1h G1(:,i)];
    end

    k2h=G1(:,Hn+1);

    for i=Hn+2:1:Hn+Hm
        k2h=[k2h G1(:,i)];
    end

    % 10 knots
    A=[ -0.0036 0.0300 0.2490 -0.0056 -0.4154 -0.0795 -9.81 0 ;
        -0.1841 -0.4456 0.3393 -0.0512 -0.1812 0.6229 0 0 ;
        0.0062 -0.0091 -0.2695 0.0066 0.2333 0.0250 0 0 ;
        0.0149 -0.0016 -0.4157 -0.0544 -0.3341 0.2726 0 9.81 ;
        0.0195 -0.0116 -0.8566 -0.0396 -0.6855 0.1429 0 0 ;
        -0.0184 -0.0204 -0.0274 0.0692 -0.3037 -0.7329 0 0 ;
        0 0 1 0 0 0 0 0 ;
        0 0 0 0 1 0 0 0 ];

    B=[ 0.0741 0.1236 -0.0007 -0.0025 ;
        -1.1351 0.0594 0.0010 0.0034 ;
        -0.0027 -0.0673 0.0003 0.0001 ;
        -0.0270 0.0027 0.1062 0.1927 ;
        -0.0309 0.0054 0.2216 0.1625 ;
        0.1570 -0.0011 0.0318 -0.4636 ;
        0 0 0 0 ;
        0 0 0 0 ] ;

    %nominal state values

    U0=5.13;
    V0=-0.01;
    W0=0.35;
    P0=0;
    Q0=0;
    R0=0;
    alphadot0=0;

end

if count==1
```

```
    A10k=Aprime;
    B10k=Bprime;

    k110=G1(:,1);
    for i=2:1:Hn
        k110=[k110 G1(:,i)];
    end

    k210=G1(:,Hn+1);

    for i=Hn+2:1:Hn+Hm
        k210=[k210 G1(:,i)];
    end

    % 20 knots
    A=[ -0.0046 0.0380 0.3259 -0.0045 -0.4020 -0.0730 -9.81 0 ;
        -0.1978 -0.5667 0.3570 -0.0378 -0.2149 0.5683 0 0 ;
        0.0039 -0.0029 -0.2947 0.0070 0.2266 0.0148 0 0 ;
        0.0133 -0.0014 -0.4076 -0.0654 -0.4093 0.2674 0 9.81 ;
        0.0127 -0.0100 -0.8152 -0.0397 -0.8210 0.1442 0 0 ;
        -0.0285 -0.0232 0.1064 0.0709 -0.2786 -0.7396 0 0 ;
        0 0 1 0 0 0 0 0 ;
        0 0 0 0 1 0 0 0 ];

    B=[ 0.0676 0.1221 -0.0001 -0.0016 ;
        -1.1151 0.1055 0.0039 0.0035 ;
        -0.0062 -0.0682 0.0000 0.0035 ;
        -0.0170 0.0049 0.1067 0.1692 ;
        -0.0129 0.0106 0.2227 0.1430 ;
        0.1390 -0.0059 0.0326 -0.4070 ;
        0 0 0 0 ;
        0 0 0 0 ] ;

    %nominal state values
    U0=10.27;
    V0=-0.01;
    W0=0.66;
    P0=0;
    Q0=0;
    R0=0;
    alphadot0=0;

end

if count==2

    A20k=Aprime;
    B20k=Bprime;

    k120=G1(:,1);

    for i=2:1:Hn
        k120=[k120 G1(:,i)];
    end
```

```
            k220=G1(:,Hn+1);

            for i=Hn+2:1:Hn+Hm
                k220=[k220 G1(:,i)];
            end

        end

        count=count+1;

    end

    CU=[1,0,0,0,0,0,0,0,0,0,0,0,0,0,0,0,0,0,0,0,0];
    sat=[13.6,16.5,16.5,8.2];
    x0=[0,0,0,0,0,0,0,0,0,0,0,0,0,0,0,0,0,0,0,0,0];
    r=[0,-0.05,0.000,0]';
    r2=[0,-0.0135,0.00,0]';
    r3=[0,0.05,0.000,0]';
    rf=[0,0.000,0.000,0]';

    sim('modelfollowb2')

end
```

Simulink program

Modelfollowb2

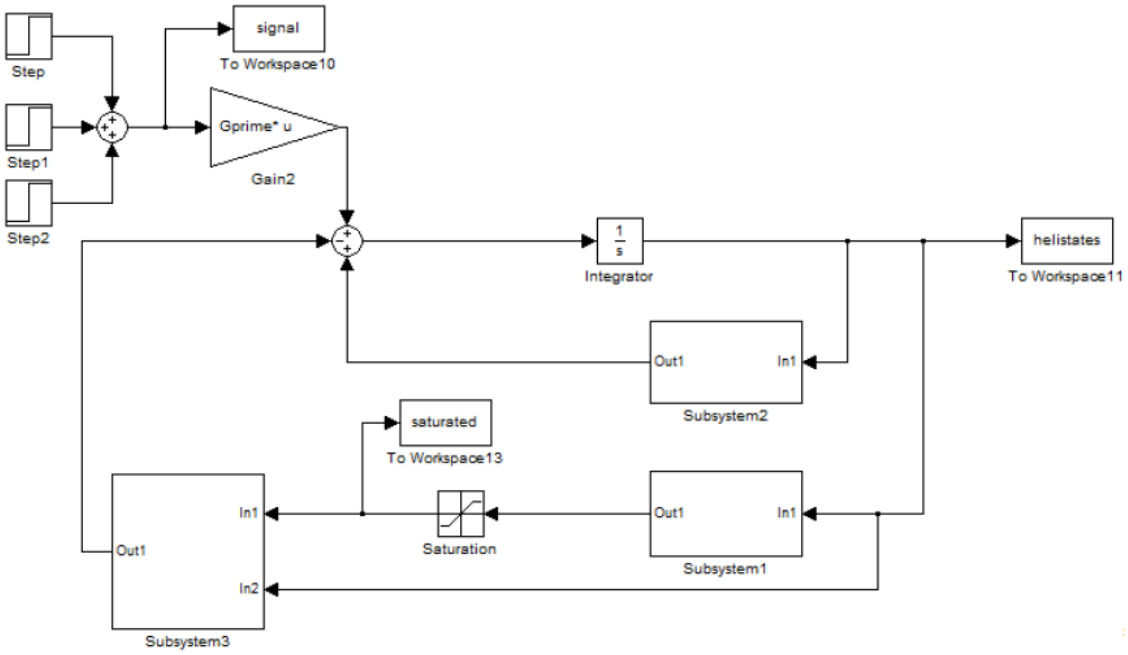

Subsystem 1

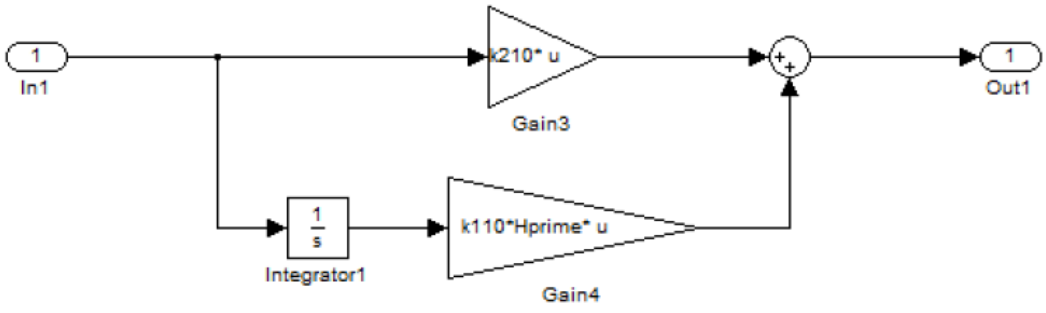

- 1 is the helicopter states

Subsystem 2

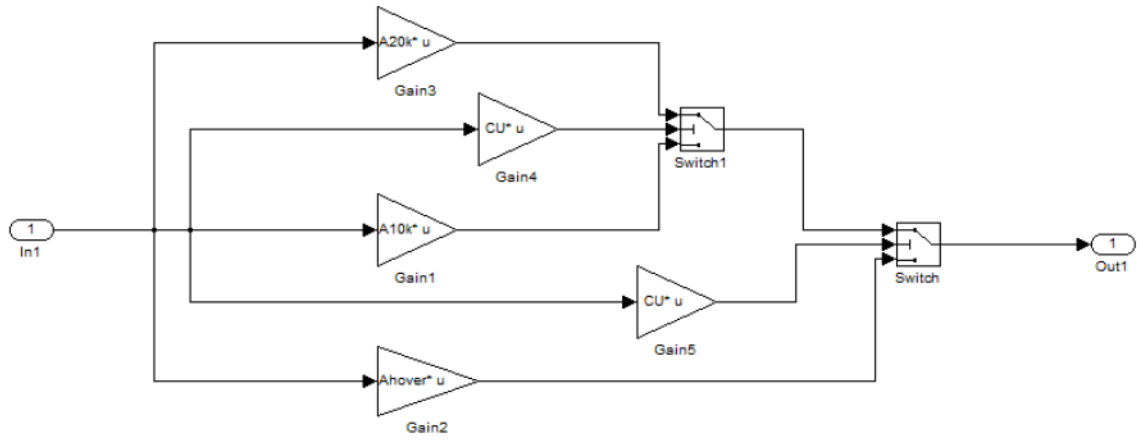

- 1 is the helicopter states
- CU is used to make the helicopter forward velocity the input 2 of the switches
- Switch 1 is set to change signal when input 2 reaches a value of 7.5
- Switch is set to change signal when input 2 reaches a value of 2.5

Subsystem 3

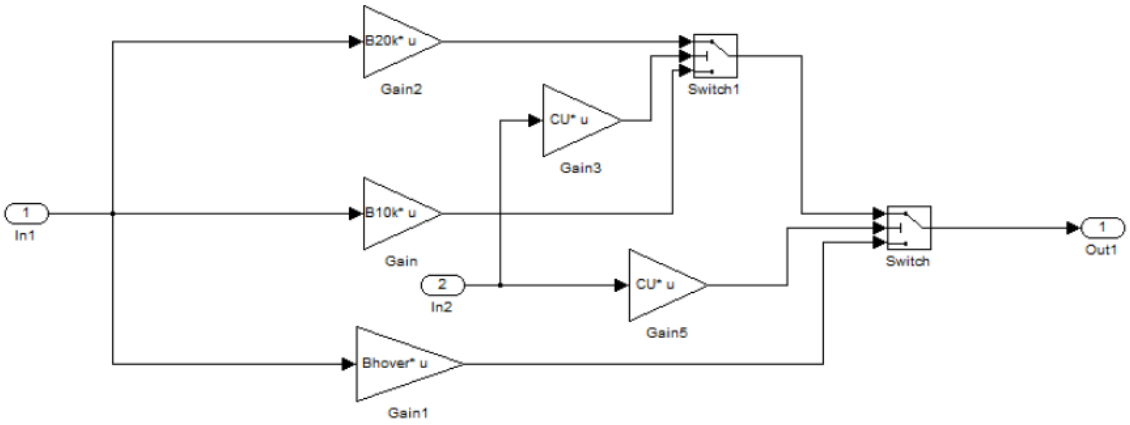

- 1 is the control signal after the saturation
- 2 is the helicopter states
- CU is used to make the helicopter forward velocity the input 2 of the switches
- Switch 1 is set to change signal when input 2 reaches a value of 7.5
- Switch is set to change signal when input 2 reaches a value of 2.5